TITLE

Population scale mapping of novel transposable element diversity reveals links to gene regulation and epigenomic variation

KEYWORDS

Epigenetics, DNA methylation, transposable elements, genomics, Arabidopsis

AUTHORS

Tim Stuart[1], Steven R. Eichten[2], Jonathan Cahn[1], Justin Borevitz[2], Ryan Lister[1]

AFFILIATIONS

1 - ARC Centre of Excellence in Plant Energy Biology, The University of Western Australia, Perth, Australia

2 - ARC Centre of Excellence in Plant Energy Biology, The Australian National University, Canberra, Australia

Corresponding author: Ryan Lister (ryan.lister@uwa.edu.au)

Author ORCID IDs:

0000-0002-3044-0897 (TS)

0000-0003-2268-395X (SRE)

0000-0002-5006-741X (JC)

0000-0001-6637-7239 (RL)

ABSTRACT

Variation in the presence or absence of transposable element (TE) insertions is a significant source of inter-individual genetic variation. Here, we identified 23,095 TE presence/absence variants between 216 wild Arabidopsis accessions. Most variants are rare, however over two thirds of the common alleles identified were not in linkage disequilibrium with nearby SNPs, implicating TE variants as a source of missing heritability. Some TE variants were associated with altered expression of nearby genes, with potential functional consequences including decreased pathogen resistance. The majority of inter-accession DNA methylation differences were associated with nearby TE variants, indicating an important role in facilitating epigenomic variation. Examination of TE regulation following crosses between parents with differential TE content revealed that absence of individual TEs from the paternal genome is associated with DNA demethylation within maternal copies of these TEs in the embryo, suggesting parental TE variation may enable activation of previously silent TEs.

INTRODUCTION

Transposable elements (TEs) are mobile genetic elements present in nearly all studied organisms, and make up a large fraction of most eukaryotic genomes. The two classes of TEs are retrotransposons (class I elements), which transpose via an RNA intermediate requiring a reverse transcription reaction, and DNA transposons (class II elements), which transpose via either a cut-paste or, in the case of Helitrons, a rolling circle mechanism with no RNA intermediate (Wicker et al. 2007). TE activity poses significant mutagenic potential because TE insertion may disrupt essential regions of the genome, and so safeguards have evolved in order to suppress this activity. These safeguards include epigenetic transcriptional silencing mechanisms, chiefly involving the methylation of cytosine nucleotides (DNA methylation) to

48 produce 5-methylcytosine (mC), a mark that can signal transcriptional silencing of the
49 methylated locus. In *Arabidopsis thaliana* (Arabidopsis), DNA methylation occurs in three DNA
50 sequence contexts: mCG, mCHG, and mCHH, where H is any base but G. Establishment of
51 DNA methylation marks can be carried out by two distinct pathways – the RNA-directed DNA
52 methylation pathway guided by 24 nucleotide (nt) small RNAs (smRNAs), and the DDM1/CMT2
53 pathway (Zemach et al. 2013; Matzke and Mosher 2014). A major function of DNA methylation
54 in Arabidopsis is in the transcriptional silencing of TEs. Loss of DNA methylation due to
55 mutations in genes essential for DNA methylation establishment and maintenance leads to
56 expression of previously silent TEs, and sometimes transposition (Mirouze et al. 2009; Miura et
57 al. 2001; Saze et al. 2003; Lippman et al. 2004; Jeddeloh et al. 1999; Zemach et al. 2013).
58 TEs are thought to play an important role in evolution, not only because of the disruptive
59 potential of their transposition. The release of transcriptional and post-transcriptional silencing of
60 TEs can lead to bursts of TE activity, quickly generating new genetic diversity on which
61 selection may act (Vitte et al. 2014). TEs may carry regulatory information such as promoters
62 and transcription factor binding sites, and their mobilization may lead to the creation or
63 expansion of gene regulatory networks (Hénaff et al. 2014; Bolger et al. 2014; Ito et al. 2011;
64 Makarevitch et al. 2015). Furthermore, the transposase enzymes required and encoded by TEs
65 have frequently been domesticated and repurposed as endogenous proteins, such as the
66 *DAYSLEEPER* gene in Arabidopsis, derived from a hAT transposase enzyme (Bundock and
67 Hooykaas 2005). Clearly, the activity of TEs can have widespread and unpredictable effects on
68 the host genome. However, the identification of TE presence/absence variants in genomes has
69 remained difficult. It is challenging to identify the structural variants caused by TE mobilization
70 using current short-read sequencing technologies as these reads are typically mapped to a
71 reference genome, which has the effect of masking structural changes that may be present.
72 However, in terms of the number of base pairs affected, a large fraction of genetic differences

between Arabidopsis accessions appear to be due to variation in TE content (Cao et al. 2011). Therefore identification of TE variants is essential in order to develop a more comprehensive understanding of the genetic variation that exists between genomes, and of the consequences of TE movement upon genome and cellular function.

The tools developed previously for identification of novel TE insertion sites have several limitations. They either require a library of active TE sequences, cannot identify TE absence variants, or are not designed with population studies in mind (Thung et al. 2014; Robb et al. 2013; Hénaff et al. 2015). In order to accurately map the locations of TE presence/absence variants with respect to a reference genome, we have developed a novel algorithm, TEPID (Transposable Element Polymorphism IDentification), which is designed for population studies. We tested our algorithm using both simulated and real Arabidopsis sequencing data, finding that TEPID is able to accurately identify TE presence/absence variants with respect to the Col-0 reference genome. We applied our TE analysis method to existing genome resequencing data for 216 different wild Arabidopsis accessions, and identified widespread TE variation amongst these accessions (Schmitz et al. 2013). The majority of these TE variants arose recently in evolutionary times, represent novel genetic variants, and are associated with a variety of epigenomic and transcriptional variation.

RESULTS

Computational identification of TE presence/absence variation

We developed TEPID, an analysis pipeline capable of detecting TE presence/absence variants from paired end DNA sequencing data. TEPID integrates split and discordant read mapping information, read mapping quality, sequencing breakpoints, as well as local variations in sequencing coverage to identify novel TE presence/absence variants with respect to a reference TE annotation (Figure 1A; see methods). After TE variant discovery has been

98 performed, TEPID then includes a second step designed for population studies. This examines
99 each region of the genome where there was a TE insertion identified in any member of the
100 group, and checks for evidence of this insertion in each member of the population. In this way,
101 TEPID leverages TE variant information for a group of related samples to correct false negative
102 calls within the group. This feature sets TEPID apart from previous similar methods for TE
103 variant discovery using short read data (Hénaff et al. 2015). Testing of TEPID using simulated
104 TE variants in the Arabidopsis genome showed that it was able to reliably detect simulated TE
105 variants (Figure 1B). In order to assess further the accuracy of TE variant discovery using
106 TEPID, we compared our predicted TE variants identified in the Landsberg *erecta* (L*er*)
107 accession with the *de novo* assembly reference genome created using long sequencing reads.
108 Previously published 100 bp paired-end L*er* genome resequencing reads (Schneeberger et al.
109 2011) were first analyzed using TEPID, enabling identification of 446 TE insertions and 758 TE
110 absence variants with respect to the Col-0 reference TE annotation (Supplementary File 1).
111 Reads providing evidence for these variants were then mapped to the L*er* reference genome
112 that was generated by *de novo* assembly using Pacific Biosciences P5-C3 chemistry with a 20
113 kb insert library (Chin et al. 2013), using the same alignment parameters as was used to map
114 reads to the Col-0 reference genome. This resulted in 98.7% of reads being aligned
115 concordantly to the L*er* reference, whereas 100% aligned discordantly or as split reads to the
116 Col-0 reference genome (Table 1). To find whether reads mapped to homologous regions in
117 both the Col-0 and L*er* reference genomes, we conducted a blast search (Camacho et al. 2009)
118 using the DNA sequence between read pair mapping locations in the L*er* genome against the
119 Col-0 genome, and found the top blast result for 80% of reads providing evidence for TE
120 insertions, and 89% of reads providing evidence for TE absence variants in L*er*, to be located
121 within 200 bp of the TE variant reported by TEPID. We conclude that reads providing evidence
122 for TE variants map discordantly or as split reads when mapped to the Col-0 reference genome,

123 but map concordantly to homologous regions of the L*er de novo* assembled reference genome,
124 indicating that structural variation is present at the sites identified by TEPID, and that this is
125 resolved in the *de novo* assembled genome.
126
127 **Abundant TE positional variation among natural Arabidopsis populations**
128 We used TEPID to analyze previously published 100 bp paired-end genome resequencing data
129 for 216 different wild Arabidopsis accessions (Schmitz et al. 2013), and identified 15,007 TE
130 insertions and 8,088 TE absence variants, totalling 23,095 unique TE variants. In most wild
131 accessions we identified 300-500 TE insertions (mean = 378; Figure 2 - figure supplement 1A)
132 and 1,000-1,500 TE absence variants (mean = 1,279; Figure 2 - figure supplement 1B), the
133 majority of which were shared by two or more accessions (Figure 2 - figure supplement 2). PCR
134 validations were performed for a random subset of 10 insertions and 10 absence variants in 14
135 accessions, and confirmed the high accuracy of TE variant discovery using the TEPID package,
136 with results similar to that observed using simulated data (Figure 1C, D). TE variants were
137 distributed throughout chromosome 1 in a pattern that is similar to the distribution of all Col-0
138 TEs, and were enriched in the pericentromeric regions (Figure 2A, figure supplement 3). This
139 distribution was also similar to that observed for regions of the genome previously identified as
140 being differentially methylated in all DNA methylation contexts (mCG, mCHG, mCHH) between
141 the wild accessions (population DMRs) (Schmitz et al. 2013). Furthermore, TE variants were
142 depleted within genes and DNase I hypersensitivity sites (Sullivan et al. 2014), while they were
143 enriched in gene flanking regions and within other annotated TEs or pseudogenes (Figure 2B).
144 We did not observe any enrichment of TE insertions within the *KNOT ENGAGED ELEMENT*
145 *(KEE)* regions (Figure 2 - figure supplement 4), indicating that these regions may not act as a
146 “TE sink” as has been previously proposed (Grob et al. 2014).

147 Among the identified TE variants, several TE superfamilies were over- or under-
148 represented compared to the number expected by chance given the overall genomic frequency
149 of different TE types (Figure 2C; Supplementary Table 1). In particular, TE variants in the
150 RC/Helitron superfamily were less numerous than expected, with an 11.5% depletion of
151 RC/Helitron elements in the set of TE variants. TEs belonging to the LTR/Gypsy superfamily
152 were more variable than expected, with a 7.5% enrichment in the set of TE variants. This was
153 unlikely to be due to a differing ability of our detection methods to identify TE variants of
154 different lengths, as the TE variants identified had a similar distribution of lengths as all
155 Arabidopsis TEs annotated in the Col-0 reference genome (Figure 2 - figure supplement 5).
156 These enrichments suggest that the RC/Helitron TEs have been relatively dormant in recent
157 evolutionary history, while the LTR/Gypsy TEs have been more active. At the family level, we
158 observed similar patterns of TE variant enrichment or depletion (Figure 2 - figure supplement 6;
159 Supplementary Table 2). As expected, this TE diversity tended to reflect the known genetic
160 relationships between accessions. We further examined Arabidopsis (Col-0) DNA sequencing
161 data from a transgenerational stress experiment to investigate the possible minimum number of
162 generations required for TE variants to arise (Jiang et al. 2014). We identified a single potential
163 TE insertion in a sample following 10 generations of single-seed descent under high salinity
164 stress conditions, and no TE variants in the control single-seed descent set. However, without
165 experimental validation it remains unclear if this represents a true variant. Therefore, we
166 conclude that TE variants likely arise at a rate less than 1 insertion in 30 generations.
167 Although thousands of TE variants were identified, it is important to classify their
168 relationship to other commonly identified sources of genetic variation such as single nucleotide
169 polymorphisms (SNPs). This comparison can determine if TE variants are often in linkage
170 disequilibrium with nearby SNPs, or if they are a previously unassessed source of genetic
171 variation between accessions unlinked to the underlying SNP-based haplotypes. To investigate

172 this relationship, SNPs previously identified between the wild accessions (Schmitz et al. 2013)
173 were compared to the presence/absence of individual TE variants. For the 7,300 testable TE
174 variants in the sample set with a minor allele frequency above 3%, the nearest 300 flanking
175 SNPs upstream and downstream of the TE insertion site were analyzed for linkage
176 disequilibrium (LD, r^2; Figure 2D-F; see methods). TE variants were classified as being either
177 'young', 'mid', or 'old' variants by comparing ranked r^2 values to flanking SNPs against the
178 median ranked r^2 value for all SNP-SNP comparisons to account for regional variation in LD
179 (Figure 2D, E). This analysis identified TE variants that were unlinked (young) or linked (old) to
180 SNPs forming local haplotypes, or were in an intermediate linkage state (mid) with their
181 surrounding haplotype. The majority (61%) of testable TE variants were largely unlinked to
182 nearby SNPs, and are therefore predicted to be young variants present in a few divergent
183 accessions (Figure 2F). In contrast, 29% of TE variants displayed high levels of linkage with
184 nearby SNPs, and are likely old insertions. TE variants displayed a similar chromosomal
185 distribution regardless of age classification (Figure 2G). Overall, this analysis revealed an
186 abundance of previously unexplored genetic variation that exists amongst Arabidopsis
187 accessions caused by the presence or absence of TEs, and illustrates the importance of
188 identifying TE variants to capture missing heritability alongside other genetic diversity such as
189 SNPs.
190

191 **TE variants affect gene expression**

192 To determine whether the TE variants identified affected nearby gene expression, we compared
193 the steady state transcript abundance within mature leaf tissue, between accessions with and
194 without TE insertions, for genes with TE variants located in the 2 kb gene upstream region, 5'
195 UTR, exon, intron, 3' UTR or 2 kb downstream region (Figure 3). While the steady state
196 transcript abundance of most genes appeared to be unaffected by the presence of a TE, 45

197 genes displayed significant differences in transcript abundance linked with the presence of a TE
198 variant, indicating a functional role for these variants in the local regulation of gene expression
199 (q-value < 0.001 with greater than 2-fold change in transcript abundance; Figure 3, Table 2). We
200 did not find any functional category enrichments in this set of differentially expressed genes. It
201 should be noted that rare TE variants, with a minor allele frequency less than 3%, may also be
202 associated with a difference in transcript abundance, but were unable to be statistically tested
203 due to their rarity. Future studies using larger sample sizes may be able to further examine the
204 frequency at which TE variants impact gene expression.

205 As both increases and decreases in transcript abundance of nearby genes were
206 observed for TE variants within each gene feature, it appears to be difficult to predict the impact
207 a TE variant may have on nearby gene expression. However, gene-level transcript abundance
208 measurements may fail to identify the potential positional effect of TE variants upon
209 transcription. To more closely examine changes in transcript abundance associated with TE
210 variants among the accessions, we inspected a subset of TE variant sites and identified TE
211 variants that appear to have an impact on transcriptional patterns beyond changes in total
212 transcript abundance. For example, the presence of a TE within an exon of *AtRLP18*
213 (AT2G15040) was associated with truncation of the transcripts at the TE insertion site in
214 accessions possessing the TE variant, as well as silencing of a downstream gene encoding a
215 leucine-rich repeat protein (AT2G15042) (Figure 4A-D). Both genes have significantly lower
216 transcript abundance in accessions containing the TE insertion ($p < 5.8 \times 10^{-10}$, Mann-Whitney U
217 test; Figure 4C). *AtRLP18* is reported to be involved in bacterial resistance, with the disruption
218 of this gene by T-DNA insertion mediated mutagenesis resulting in increased susceptibility to
219 the bacterial plant pathogen *Pseudomonas syringae* (Wang et al. 2008). We examined
220 pathogen resistance phenotype data (Aranzana et al. 2005) for accessions with and without a
221 TE insertion in the *AtRLP18* exon, and found that accessions containing the TE insertion were

222 sensitive to infection by *Pseudomonas syringae* transformed with *avrPpH3* genes at a much
223 higher frequency (Figure 4E). This suggests that the wild accessions identified here to contain a
224 TE insertion within *AtRLP18* may have an increased susceptibility to certain bacterial
225 pathogens.

226 We also observed some TE variants associated with increased expression of nearby
227 genes. For example, presence of a TE within the upstream region of a gene encoding a
228 pentatricopeptide repeat (PPR) protein (AT2G01360) was associated with higher steady state
229 transcript abundance of this gene (Figure 4F-H). Interestingly, transcription appeared to begin at
230 the TE insertion point, rather than the transcriptional start site of the gene (Figure 4F).
231 Accessions containing the TE insertion had significantly higher AT2G01360 transcript
232 abundance than the accessions without the TE insertion ($p < 1.8 \times 10^{-7}$, Mann-Whitney U test;
233 Figure 4H). The apparent transcriptional activation, linked with presence of a TE belonging to
234 the *HELITRON1* family, indicates that this element may carry sequences or other regulatory
235 information that has altered the expression of genes downstream of the TE insertion site.
236 Importantly, this variant was classified as a young TE insertion, as it is not in linkage
237 disequilibrium with surrounding SNPs, and therefore the associated changes in gene transcript
238 abundance would not be identified using only SNP data. This TE variant was also upstream of
239 *QPT* (AT2G01350), involved in NAD biosynthesis (Katoh et al. 2006), which did not show
240 alterations in steady state transcript abundance associated with the presence of the TE variant,
241 indicating a potential directionality of regulatory elements carried by the TE (Figure 4G, H).
242 Overall, these examples demonstrate that TE variants can have unpredictable, yet important,
243 effects of the expression of nearby genes, and these effects may be missed by studies focused
244 on genetic variation at the level of SNPs.

245

246 **TE variants drive DNA methylation differences between accessions**

247 As TEs are frequently highly methylated in Arabidopsis (Lister et al. 2008; Cokus et al. 2008;
248 Zhang et al. 2006; Zilberman et al. 2007), we next assessed the DNA methylation state
249 surrounding TE variant sites to determine whether TE variants might be responsible for some of
250 the differences in DNA methylation patterns previously observed between the wild accessions
251 (Schmitz et al. 2013). We found that 61% of the 13,485 previously reported population DMRs
252 were located within 1 kb of a TE variant, significantly more than expected by chance ($p < 1 \times 10^{-}$
253 ^{4}, determined by resampling 10,000 times; Figure 5A). Old TE variants were more often located
254 close to population DMRs, with 41.5% of TE variants within 1 kb of a population DMR classified
255 as old, 11.5% higher than the total genomic frequency of old elements (Figure 5B). There was a
256 corresponding depletion of young TE variants in this set, with 48.5% being classified as young,
257 11.5% lower than the total genomic frequency of young TE variants. This indicates that
258 established TE insertions may be more important than recent TE insertions in defining DNA
259 methylation landscapes. Alternatively, unmethylated TEs may be preferentially lost from the
260 population due to selection, resulting in old TE variants being more highly methylated. DNA
261 methylation levels at population DMRs located within 1 kb a TE variant, henceforth termed TE-
262 DMRs, were positively correlated with the presence of the TE variant (Figure 5C), while DNA
263 methylation levels at population DMRs further than 1 kb from a TE variant did not have a
264 significant association with the presence/absence of the nearest TE variant. TE-DMRs were
265 significantly more highly methylated in accessions containing the TE, suggesting that TE
266 variants may facilitate changes in DNA methylation patterns between accessions (Welch's t-
267 test, $p < 2.2 \times 10^{-16}$; Figure 5D). Overall, this indicates that a large fraction of the population
268 DMRs previously identified between these accessions are associated with the presence of local
269 TE insertions.

270 We next examined levels of DNA methylation in regions flanking all TE insertions
271 regardless of the presence or absence of a population DMR call, and similarly found that

272 accessions containing a TE insertion had a highly localized enrichment in DNA methylation in all
273 sequence contexts (Figure 5E, F), again indicating that TE variants may play a role in shaping
274 DNA methylation landscapes between Arabidopsis accessions. As the increase in DNA
275 methylation around TE insertion sites appeared to be restricted to regions >200 bp from the
276 insertion site, we correlated DNA methylation levels in 200 bp regions flanking TE variants with
277 the presence/absence of TE variants. DNA methylation levels were positively correlated with the
278 presence of a TE (Figure 5G). Furthermore, DNA methylation level was more strongly
279 correlated with the presence of old TE variants. These results indicate that DNA methylation
280 patterns are influenced by the differential TE content of individual genomes, and that the DNA
281 methylation-dependent silencing of TE variants may lead to formation of DMRs between wild
282 Arabidopsis accessions. The age of TE variants also appears to be related to the DNA
283 methylation state surrounding the TE insertion site, with older variants being more highly
284 methylated, suggesting that many generations may be required before a new TE insertion
285 reaches a highly methylated state.
286
287 **TE regulation in the germline**
288 To explore when during development germline changes in TE content may occur, we sought to
289 associate TE DNA methylation dynamics during germline development and early
290 embryogenesis with the differential TE content we observe between the different Arabidopsis
291 accessions. Complex DNA methylation changes occur in the Arabidopsis germline, particularly
292 within TE sequences. During male germline development, the haploid microspore undergoes
293 asymmetric division to produce the larger vegetative cell and a smaller cell that divides once
294 more to produce two identical sperm cells (Figure 6A) (Kawashima and Berger 2014). Some
295 TEs have previously been found to become transcriptionally active and to transpose in the
296 vegetative cell nucleus (VN). This TE activation has been linked to an increase in 21 nt smRNAs

297 derived from activated TE sequences, that are thought to then be transported to the sperm cells
298 (Slotkin et al. 2009). In contrast, the sperm and post-meiotic microspore genomes lose DNA
299 methylation in the mCHH context within many TEs due to decreased DRM2 abundance but are
300 able to maintain TE silencing (Slotkin et al. 2009; Calarco et al. 2012). A largely distinct set of
301 TEs are demethylated in the mCG context in the VN compared to the microspore and sperm
302 cells, and are thought to be involved in epigenetic imprinting rather than TE silencing (Calarco et
303 al. 2012). In the female germline, the ovule contains a diploid central cell and haploid egg cell.
304 As in the VN, the non-generative central cell acts as a companion to the egg and expresses
305 *DEMETER*, which encodes a DNA demethylase, resulting in global DNA demethylation (Ibarra
306 et al. 2012). During fertilization, one sperm fertilizes the egg to form the diploid embryo, while
307 the other sperm fertilizes the diploid central cell to form the triploid endosperm, which supplies
308 nutrients to the developing embryo (Figure 6A) (Kawashima and Berger 2014). The endosperm
309 remains globally demethylated, while DNA methylation is gradually restored in the embryo
310 through RdDM (Jullien et al. 2012; Hsieh et al. 2009).

311 In order to determine whether these TEs that undergo DNA methylation changes in the
312 male germline or in the embryo and endosperm are especially active elements, we examined
313 both the number of unique insertions caused by these differentially methylated elements
314 (transposition frequency), as well as the presence/absence variability of these TEs among the
315 wild accessions (Figure 6B, C) (Hsieh et al. 2009; Calarco et al. 2012). We found that 68% of
316 TEs previously found to be demethylated in the mCHH context in Col-0 sperm and microspore
317 were absent from non-Col-0 accessions (Figure 6B), a much larger fraction than expected by
318 chance ($p < 1 \times 10^{-4}$, determined by resampling 10,000 times) (Calarco et al. 2012). In contrast,
319 TEs differentially methylated in the mCG context in the sperm or microspore, thought to be
320 involved in epigenetic imprinting, or in the mCHH context in the developing embryo (Hsieh et al.
321 2009), were not absent from non-Col-0 accessions significantly more often than expected ($p >$

322 0.09, determined by resampling 10,000 times; Figure 6B). While TEs mCG-hypomethylated in
323 the endosperm were absent from non-Col-0 genomes significantly more often than expected (p
324 $< 1 \times 10^{-4}$, determined by resampling 10,000 times), the scale of this difference was small, with
325 only 30% of the TEs absent in non-Col-0 accessions. mCHH-demethylated TEs in the sperm
326 and microspore also had a significantly higher transposition frequency, suggesting that they
327 have been more active than most other TEs in the Arabidopsis genome (Figure 6C; Welch's t-
328 test, $p < 1 \times 10^{-5}$). While mCHH-hypermethylated TEs in the embryo were not found to be
329 frequently absent from non-Col-0 accessions, these elements did show a significantly higher
330 transposition frequency, as did elements mCG-hypomethylated in the endosperm, indicating
331 that demethylation of active TEs in the germline companion cells (the VN and endosperm) may
332 be important in driving DNA methylation changes in the generative cells (the sperm and
333 embryo), perhaps acting to suppress transposition of active elements in the germline.

334 TEs that are demethylated in the mCHH context in the developing sperm may rely on
335 smRNAs in the seed for the restoration of proper DNA methylation of paternal TE sequences in
336 the embryo following fertilization, through RdDM (Jullien et al. 2012). These smRNAs are
337 thought to be maternally-derived, and are likely produced in the endosperm (Mosher et al. 2009;
338 Calarco et al. 2012). We sought to determine whether TEs present in only one parental genome
339 in an intraspecific cross would show altered levels of smRNAs targeted to these TEs, as the
340 absence of a TE in the maternal genome may lead to the loss of a maternally-derived smRNA
341 signal in the seed. Using previously published whole seed 21-24 nt smRNA data for reciprocal
342 crosses between Col-0 and Cvi or L*er* (Pignatta et al. 2014; Gehring et al. 2014), we examined
343 seed smRNA levels in TEs present in the Col-0 genome but absent from the Cvi genome for
344 crosses between Col-0 and Cvi, or absent from the L*er* genome for crosses between Col-0 and
345 L*er* (Figure 6D, direction of each cross is depicted as *female x male* on axis labels). Consistent
346 with previous reports, we found that smRNA levels in TEs were dependent on maternal

347 genotype but independent of paternal genotype, indicating that they are maternally-derived.
348 Furthermore, we confirmed that TEs present in only the paternal genome in a cross had
349 significantly lower 21-24 nt smRNA levels compared with crosses where the TE was present in
350 the maternal genome ($p < 1.4 \times 10^{-10}$, Mann-Whitney U test; Figure 6E). As these smRNAs are
351 thought to be required for TE silencing in the embryo (Jullien et al. 2012; Matzke and Mosher
352 2014), this may then lead to TE activation and may explain the higher transposition frequencies
353 we observe for TEs demethylated in the mCHH context in the sperm genome.

354 To test whether the absence of a TE in the maternal genome was sufficient to prevent
355 the re-methylation of the paternal copy of that TE following fertilization, we examined previously
356 published embryonic DNA methylation data within Cvi-absent TEs following reciprocal crosses
357 between Col-0 and Cvi (Pignatta et al. 2014) (Figure 6F). For all crosses between Col-0 and
358 Cvi, Cvi-absent TEs showed significantly lower mCG levels, and this is likely due to the global
359 reduction in mCG levels that exists in the Cvi genome rather than the absence of the TE in one
360 parent (Pignatta et al. 2014). Surprisingly, we found for TEs that lose mCHH in the sperm
361 (Calarco et al. 2012), when the TE was absent from the maternal genome (Cvi x Col-0),
362 embryonic mCHH levels within these TEs were not significantly different from DNA methylation
363 levels in the Col-0 x Col-0 cross, where the TE was present in both parents ($p > 0.04$, Mann-
364 Whitney U test; Figure 6F). This was contrary to the anticipated pattern, where the loss of
365 maternal smRNAs observed for this cross (Figure 6E) would prevent these sperm-demethylated
366 TEs from being re-methylated in the embryo, and may indicate that maternally-derived smRNAs
367 are not essential for establishing DNA methylation patterns in early embryonic development.
368 However, when the parents were reversed and the TE variants were present in the maternal
369 genome but absent from the paternal genome (Col-0 x Cvi), we found a significant reduction in
370 mCHH methylation for these TEs, indicating that paternal signals may be required for DNA
371 methylation of maternal TE sequences ($p < 5 \times 10^{-7}$, Mann-Whitney U test). To further

372 investigate this result, we analyzed an independent dataset containing embryonic DNA
373 methylation data for crosses between Col-0 and L*er*, generated at a slightly later developmental
374 stage (7-8 days after pollination) than the data for crosses between Col-0 and Cvi (6 days after
375 pollination). Within TEs absent from L*er* and demethylated in the Col-0 sperm (Ibarra et al.
376 2012) we found no significant difference in DNA methylation levels in any context dependent on
377 the parental genotypes (Figure 6 - figure supplement 1). This could indicate that embryonic DNA
378 methylation changes within maternal TEs, dependent upon paternal genotype, may be restricted
379 to early developmental time points, less than 6 days after pollination, or may be dependent on
380 the intraspecific cross performed.

381 Considering the high proportion of sperm mCHH-demethylated TEs that were found to
382 be absent in non-Col-0 accessions (Figure 6B), crosses between plants with differential
383 presence/absence of these TEs may be possible in the wild, and such crosses may lead to the
384 demethylation of the maternal copies of these TEs in the embryo when a paternal copy is
385 absent. These findings support a model for TE silencing escape facilitated by genetic
386 differences between parents, as the loss of DNA methylation within TEs has been shown
387 previously to be sufficient for transcriptional activation and transposition of demethylated TEs
388 (Gendrel et al. 2002; Hirochika et al. 2000; Stroud et al. 2013). Such mating situations may also
389 lead to the formation of stable epialleles depending of the length of time the TE sequences are
390 able to escape remethylation, and this may play a role in formation of the patterns of differential
391 DNA methylation previously observed between wild accessions (Schmitz et al. 2013).

392

393 **DISCUSSION**

394 Here, we discovered widespread differential TE content between wild Arabidopsis accessions. A
395 subset (32%) of TE variants with a minor allele frequency above 3% were able to be tested for
396 linkage with nearby SNPs. The majority of these TE variants were unlinked to surrounding

397 SNPs, indicating that they represent genetic variants currently overlooked in genomic studies.
398 We found a marked depletion of TE variants within gene bodies and DNase I hypersensitivity
399 sites, indicating that the more deleterious TE insertions have likely been removed from this
400 population through selection. Importantly, we were able to identify examples where TE variants
401 appear to have an effect upon gene expression, both in the disruption of transcription and in the
402 spreading or disruption of regulatory information leading to the transcriptional activation of
403 genes, indicating that these TE variants can have important consequences upon expression of
404 protein coding genes. Furthermore, we provide evidence that differential TE content between
405 genomes of wild Arabidopsis accessions underlies a large fraction of the previously reported
406 DNA methylation differences between accessions. Thus, the frequency of pure epialleles,
407 independent of underlying genetic variation, may be even more rare than previously anticipated
408 (Richards 2006). The level of DNA methylation changes associated with TE variants is related
409 to TE age, with old variants being more strongly correlated with increased DNA methylation
410 levels. This suggests that the methylation of new TE insertions is a gradual process that occurs
411 incrementally over many generations, or that unmethylated TEs are preferentially lost from the
412 population over time.

413 Identification of TE variants between Arabidopsis accessions has also enabled a closer
414 examination of the changes in TE smRNA and DNA methylation levels following fertilization of
415 intraspecific hybrids. smRNA levels in the seed appear to be dependent on maternal genome
416 content, as the presence of a TE in only the paternal genome of a cross is associated with
417 decreased levels of corresponding 21-24 nt smRNAs derived from those TEs in the seed. This
418 loss of smRNAs, dependent on maternal genotype, is strikingly similar to findings from studies
419 performed in *Drosophila melanogaster* over 3 decades ago, where maternal absence of
420 paternal *P* elements in a cross was found to lead to activation and frequent transposition of
421 these *P* elements, due to absence of maternally-derived smRNA signals needed for TE

422 silencing, while TE activation was not observed when the *P* elements were present in the
423 maternal genome (Bingham et al. 1982; Blumenstiel and Hartl 2005). This is thought to be the
424 underlying cause of hybrid dysgenesis, a phenotype characterised by sterility and high rates of
425 germline TE activity, and where the transpositions caused by active *P* elements are often lethal
426 to the hybrid offspring. It has been hypothesized previously that a process similar to Drosophila
427 hybrid dysgenesis may occur in Arabidopsis, as smRNAs in the Arabidopsis seed also appear
428 to be maternally-derived, and there is some prior evidence that this may be true (Martienssen
429 2010). Interspecific crosses between *Arabidopsis thaliana* females and *Arabidopsis arenosa*
430 males was observed to lead to the expression of previously silent paternal *ATHILA* TEs, thought
431 to be due to the presence of *ATHILA* elements in the *A. arenosa* genome that are absent from
432 the *A. thaliana* genome (Josefsson et al. 2006). However, the reciprocal cross is impossible to
433 generate due to pollination failure, constituting a fundamental limitation of this system for
434 studying hybrid dysgenesis. The use of wild *A. thaliana* accessions may prove more fruitful in
435 future experiments aiming to elucidate the processes of germline TE regulation in plants.

436 Surprisingly, we found that this decrease in smRNA levels targeting paternal TE
437 sequences was not linked to DNA demethylation of the corresponding paternal TEs in the
438 embryo, but instead observed an inverse relationship, where TEs absent from the paternal
439 genome in a cross were linked with embryonic demethylation of the maternal copy. This
440 indicates that maternal smRNAs are not essential for restoring the paternal patterns of DNA
441 methylation that are erased in the sperm, nor are they sufficient to maintain DNA methylation
442 within maternal TEs in the absence of paternal TE copies. As 21 nt smRNA production is greatly
443 increased within the pollen VN, and these smRNAs may be transported to the sperm cells
444 (Slotkin et al. 2009), it is possible that these paternal smRNAs remain present in the sperm
445 cytoplasm during fertilization. These smRNAs may play an important role in establishing early
446 patterns of DNA methylation in the embryo, perhaps explaining the non-reliance of paternal TE

447 sequences upon maternal smRNAs. This issue is somewhat complicated by the lack of embryo-
448 specific smRNA data, as all existing data have been generated from whole seed. If maternal
449 smRNAs are produced and remain in the endosperm rather than the embryo, this could further
450 explain the apparent reliance upon paternal silencing signals for proper establishment of DNA
451 methylation patterns following fertilization. Our data provides the first evidence that embryonic
452 TE silencing in Arabidopsis may be dependent on paternal, rather than maternal, silencing
453 factors.

454 DNA methylation changes triggered by genetic differences between parents clearly
455 occur in Arabidopsis, although perhaps via a different mechanism as is responsible for causing
456 hybrid dysgenesis in Drosophila. These DNA methylation changes that occur in the embryo may
457 play an important role in the formation of DNA methylation differences between wild Arabidopsis
458 accessions, depending on the length of time these changes are able to persist in hybrid
459 progeny. If the loss of DNA methylation within maternal TEs that we observe is able to persist in
460 hybrid plants, this may lead to the formation of stable epialleles as the demethylated TE copy is
461 propagated through the population. Further experiments will be required to determine the
462 stability of these embryonic changes in DNA methylation that occur in hybrid plants.
463 Alternatively, if these DNA methylation changes are limited to a small developmental window,
464 perhaps less than 6 days after pollination, there may only be a short period of time where TE
465 silencing is lost and TE activation can occur, leading to new TE insertions in the early embryo.
466 Overall, our results show that TE presence/absence variants between wild Arabidopsis
467 accessions can be linked to many DNA methylation changes previously observed in the
468 population, and can have important consequences upon nearby gene expression. Furthermore,
469 the differential TE content between parents can lead to DNA methylation changes in the early
470 embryo, and could lead to activation of these elements.
471

METHODS

TEPID development

Mapping

FASTQ files are mapped to the reference genome using the 'tepid-map' algorithm (Figure 1A). This first calls bowtie2 (Langmead and Salzberg 2012) with the following options: '--local', '--dovetail', '--fr', '-R5', '-N1'. Soft-clipped and unmapped reads are extracted using Samblaster (Faust and Hall 2014), and remapped using the split read mapper Yaha (Faust and Hall 2012), with the following options: '-L 11', '-H 2000', '-M 15', '-osh'. Split reads are extracted from the Yaha alignment using Samblaster (Faust and Hall 2014). Alignments are then converted to bam format, sorted, and indexed using samtools (Li et al. 2009).

TE variant discovery

The 'tepid-discover' algorithm examines mapped bam files generated by the 'tepid-map' step to identify TE presence/absence variants with respect to the reference genome. Firstly, mean sequencing coverage, mean library insert size, and standard deviation of the library insert size is estimated. Discordant read pairs are then extracted, defined as mate pairs that map more than 4 standard deviations from the mean insert size from one another, or on separate chromosomes.

To identify TE insertions with respect to the reference genome, split read alignments are first filtered to remove reads where the distance between split mapping loci is less than 5 kb, to remove split reads due to small indels, or split reads with a mapping quality (MAPQ) less than 5. Split and discordant read mapping coordinates are then intersected using pybedtools (Dale et al. 2011; Quinlan and Hall 2010) with the Col-0 reference TE annotation, requiring 80% overlap between TE and read mapping coordinates. To determine putative TE insertion sites, regions are then identified that contain independent discordant read pairs aligned in an orientation

497 facing one another at the insertion site, with their mate pairs intersecting with the same TE
498 (Figure 1A). The total number of split and discordant reads intersecting the insertion site and the
499 TE is then calculated, and a TE insertion predicted where the combined number of reads is
500 greater than a threshold determined by the average sequencing depth over the whole genome
501 (1/10 coverage if coverage is greater than 10, otherwise a minimum of 2 reads). Alternatively, in
502 the absence of discordant reads mapped in orientations facing one another, the required total
503 number of split and discordant reads at the insertion site linked to the inserted TE is set higher,
504 requiring twice as many reads.

505 To identify TE absence variants with respect to the reference genome, split and
506 discordant reads separated >20 kb from one another are first removed, as 99.9% of Arabidopsis
507 TEs are shorter than 20 kb, and this removes split reads due to larger structural variants not
508 related to TE diversity (Figure 2 - figure supplement 5). Col-0 reference annotation TEs that are
509 located within the genomic region spanned by the split and discordant reads are then identified.
510 TE absence variants are predicted where at least 80% of the TE sequence is spanned by a split
511 or discordant read, and the sequencing depth within the spanned region is <10% the
512 sequencing depth of the 2 kb flanking sequence, and there are a minimum number of split and
513 discordant reads present, determined by the sequencing depth (1/10 coverage; Figure 1A). A
514 threshold of 80% TE sequence spanned by split or discordant reads is used, as opposed to
515 100%, to account for misannotation of TE sequence boundaries in the Col-0 reference TE
516 annotation, as well as TE fragments left behind by DNA TEs during cut-paste transposition (TE
517 footprints) that may affect the mapping of reads around annotated TE borders (Plasterk 1991).
518 This was found to improve TE absence detection using simulated data. Furthermore, the
519 coverage within the spanned region may be more than 10% that of the flanking sequence, but in
520 such cases twice as many split and discordant reads are required. If multiple TEs are spanned
521 by the split and discordant reads, and the above requirements are met, multiple TEs in the

522 same region can be identified as absent with respect to the reference genome. Absence
523 variants in non-Col-0 accessions are subsequently recategorized as TE insertions present in the
524 Col-0 genome but absent from a given wild accession.
525
526 *TE variant refinement*
527 Once TE insertions are identified using the 'tepid-map' and 'tepid-discover' algorithms, these
528 variants can be refined if multiple related samples are analysed. The 'tepid-refine' algorithm is
529 designed to interrogate regions of the genome in which a TE insertion was discovered in other
530 samples but not the sample in question, and check for evidence of that TE insertion in the
531 sample using lower read count thresholds compared to the 'tepid-discover' step. In this way, the
532 refine step leverages TE variant information for a group of related samples to reduce false
533 negative calls within the group. This distinguishes TEPID from other similar methods for TE
534 variant discovery utilizing short sequencing reads. A file containing the coordinates of each
535 insertion, and a list of sample names containing the TE insertion must be provided to the 'tepid-
536 refine' algorithm, which this can be generated using the 'merge_insertions.py' script included in
537 the TEPID package. Each sample is examined in regions where there was a TE insertion
538 identified in another sample in the group. If there is a sequencing breakpoint within this region
539 (no continuous read coverage spanning the region), split reads mapped to this region will be
540 extracted from the alignment file and their coordinates intersected with the TE reference
541 annotation. If there are split reads present at the variant site that are linked to the same TE as
542 was identified as an insertion at that location, this TE insertion is recorded in a new file as being
543 present in the sample in question. If there is no sequencing coverage in the queried region for a
544 sample, an "NA" call is made indicating that it is unknown whether the particular sample
545 contains the TE insertion or not.
546

547 While the above description relates specifically to use of TEPID for identification of TE variants
548 in Arabidopsis in this study, this method can be also applied to other species, with the only
549 prerequisite being the annotation of TEs in a reference genome and the availability of paired-
550 end DNA sequencing data.
551
552 **TE variant simulation**
553 To test the sensitivity and specificity of TEPID, 100 TE insertions (50 copy-paste transpositions,
554 50 cut-paste transpositions) and 100 TE absence variants were simulated in the Arabidopsis
555 genome using the RSVSim R package, version 1.7.2 (Bartenhagen and Dugas 2013), and
556 synthetic reads generated from the modified genome at various levels of sequencing coverage
557 using wgsim (Li et al. 2009) (https://github.com/lh3/wgsim). These reads were then used to
558 calculate the true positive, false positive, and false negative TE variant discovery rates for
559 TEPID at various sequencing depths, by running 'tepid-map' and 'tepid-discover' using the
560 simulated reads with the default parameters (Figure 1B).
561
562 **L*er* TE analysis**
563 Previously published 100 bp paired end sequencing data for L*er*
564 (http://1001genomes.org/data/MPI/MPISchneeberger2011/releases/current/Ler-1/Reads/;
565 Schneeberger et al. 2011) was downloaded and analyzed with the TEPID package to identify
566 TE variants. Reads providing evidence for TE variants were then mapped to the *de novo*
567 assembled L*er* genome (Chin et al. 2013). To determine whether reads mapped to homologous
568 regions of the L*er* and Col-0 reference genome, the *de novo* assembled L*er* genome sequence
569 between mate pair mapping locations in L*er* were extracted, with repeats masked using
570 RepeatMasker with RepBase-derived libraries and the default parameters (version 4.0.5,
571 http://www.repeatmasker.org). A blastn search was then conducted against the Col-0 genome

572 using the following parameters: '-max-target-seqs 1', '-evalue 1e-6' (Camacho et al. 2009).
573 Coordinates of the top blast hit for each read location were then compared with the TE variant
574 sites identified using those reads.
575
576 **Arabidopsis TE variant discovery**
577 We ran the TEPID, including the insertion refinement step, on previously published sequencing
578 data for 216 different Arabidopsis populations (NCBI SRA SRA012474; Schmitz et al. 2013),
579 mapping to the TAIR10 reference genome and using the TAIR9 TE annotation. The '--mask'
580 option was also used to mask the mitochondrial and plastid genomes. We also ran TEPID using
581 previously published transgenerational data for salt stress and control conditions (NCBI SRA
582 SRP045804; Jiang et al. 2014), using the '--mask' option to mask mitochondrial and plastid
583 genomes, and the '--strict' option for highly related samples.
584
585 **TE variant / SNP comparison**
586 SNP information for 216 Arabidopsis accessions was obtained from the 1001 genomes data
587 center (http://1001genomes.org/data/Salk/releases/2013_24_01/; Schmitz et al. 2013). This was
588 formatted into reference (Col-0 state), alternate, or NA calls for each SNP. Accessions with both
589 TE variant information and SNP data were selected for analysis. Hierarchical clustering of
590 accessions by SNPs as well as TE variants were used to identify essentially clonal accessions,
591 as these would skew minor allele frequency calculations. A single representative from each
592 cluster of similar accessions was kept, leading to a total of 187 accessions for comparison. For
593 each TE variant with minor-allele-frequency greater than 3%, the nearest 300 upstream and 300
594 downstream SNPs with a minor-allele-frequency greater than 3% were selected. Pairwise
595 genotype correlations (r^2 values) for all complete cases were obtained for SNP-SNP and SNP-
596 TE variant states. r^2 values were then ordered by decreasing rank and a median SNP-SNP rank

597 value was calculated. For each of the 600 ranked surrounding positions, the number of times
598 the TE rank was greater than the SNP-SNP median rank was calculated as a relative 'age'
599 metric of TE to SNP. TE variants with less than 200 ranks over the SNP-SNP median were
600 classified as 'young' insertions. Mid-age TE variants had ranks between 200 and 400, while TE
601 variants with greater than 400 ranks above their respective SNP-SNP median value were
602 classified as 'old' variants.
603
604 **PCR validations**
605 *Selection of accessions to be genotyped*
606 To assess the accuracy of TE variant calls in accessions with a range of sequencing depths of
607 coverage, we grouped accessions into quartiles based on sequencing depth of coverage and
608 randomly selected a total of 14 accessions for PCR validations from these quartiles. DNA was
609 extracted for these accessions using Edward's extraction protocol (Edwards et al. 1991), and
610 purified prior to PCR using AMPure beads.
611
612 *Selection of TE variants for validation and primer design*
613 Ten TE insertion sites and 10 TE absence sites were randomly selected for validation by PCR
614 amplification. Only insertions and absence variants that were variable in at least two of the
615 fourteen accessions selected to be genotyped were considered. For insertion sites, primers
616 were designed to span the predicted TE insertion site. For TE absence sites, two primer sets
617 were designed; one primer set to span the TE, and another primer set with one primer
618 annealing within the TE sequence predicted to be absent, and the other primer annealing in the
619 flanking sequence (Figure 1C). Primer sequences were designed that did not anneal to regions
620 of the genome containing previously identified SNPs in any of the 216 accessions (Schmitz et
621 al. 2013) or small insertions and deletions, identified using lumpy-sv with the default settings

622 (Layer et al. 2014)(https://github.com/arq5x/lumpy-sv), had an annealing temperature close to
623 52ºC calculated based on nearest neighbor thermodynamics (MeltingTemp submodule in the
624 SeqUtils python module; Cock et al. 2009), a GC content between 40% and 60%, and contained
625 the same base repeated not more than four times in a row. Primers were aligned to the TAIR10
626 reference genome using bowtie2 (Langmead and Salzberg 2012) with the '-a' flag set to report
627 all alignments, and those with more than 5 mapping locations in the genome were then
628 removed.
629
630 *PCR*
631 PCR was performed with 10 ng of extracted, purified Arabidopsis DNA using Taq polymerase.
632 PCR products were analysed by agarose gel electrophoresis. Col-0 was used as a positive
633 control, water was added to reactions as a negative control.
634
635 **mRNA analysis**
636 Processed mRNA data for 144 wild Arabidopsis accessions were downloaded from NCBI GEO
637 GSE43858 (Schmitz et al. 2013). To find differential gene expression dependent on TE
638 presence/absence variation, we first filtered TE variants to include only those where the TE
639 variant was shared by at least 5 accessions with RNA data available, corresponding to a minor
640 allele frequency above 3%. We then grouped accessions based on TE presence/absence
641 variants, and performed a Mann-Whitney U test to determine differences in RNA transcript
642 abundance levels between the groups. We used q-value estimation to correct for multiple
643 testing, using the R qvalue package v2.2.2 with the following parameters: lambda = seq(0, 0.6,
644 0.05), smooth.df = 4 (Storey and Tibshirani 2003). Genes were defined as differentially
645 expressed where there was a greater than 2-fold difference in expression between the groups,

646 with a q-value less than 0.001. Gene ontology enrichment analysis was performed using DAVID
647 (https://david.ncifcrf.gov/).
648
649 **DNA methylation data analysis**
650 Processed DNA methylation data for wild Arabidopsis accessions were downloaded from NCBI
651 GEO GSE43857 (Schmitz et al. 2013). Weighted embryo DNA methylation data in 300 bp
652 windows for Col-0 crosses with Cvi 6 days after pollination were downloaded from the Dryad
653 Digital Repository; http://dx.doi.org/10.5061/dryad.gv536.2 (Gehring et al. 2014). Processed
654 embryo DNA methylation data in 50 bp windows for crosses between Col-0 and L*er* 7-8 days
655 after pollination were downloaded from NCBI GEO GSE38935 (Ibarra et al. 2012).
656
657 **Small RNA data analysis**
658 Normalized 21-24 nt smRNA read counts (reads per million reads mapped; RPM) in 300 bp
659 windows for whole seed 6 days after pollination, for reciprocal crosses between Col-0, Cvi, and
660 L*er* were downloaded from the Dryad Digital Repository; http://dx.doi.org/10.5061/dryad.gv536.2
661 (Gehring et al. 2014).
662

663 # DATA ACCESS

664 TEPID source code can be accessed at https://github.com/ListerLab/TEPID. L*er* TE variants are
665 available in Supplementary File 1. TE variants identified among the 216 wild Arabidopsis
666 accessions resequenced by Schmitz et al. (2013) are available in Supplementary File 2.
667

668 # ACKNOWLEDGMENTS

669 This work was supported by the Australian Research Council (ARC) Centre of Excellence
670 program in Plant Energy Biology CE140100008 (J.B., R.L.). R.L. was supported by an ARC
671 Future Fellowship (FT120100862) and Sylvia and Charles Viertel Senior Medical Research
672 Fellowship, and work in the laboratory of R.L. was funded by the Australian Research Council.
673 T.S. was supported by the Jean Rogerson Postgraduate Scholarship. S.R.E. was supported by
674 an Australian Research Council Discovery Early Career Research Award (DE150101206). We
675 thank Robert J. Schmitz, Mathew G. Lewsey, Ronan C. O'Malley, and Ian Small for their critical
676 reading of the manuscript. We also thank Kevin Murray for his helpful comments regarding the
677 development of TEPID.
678

679 ## AUTHOR CONTRIBUTIONS

680 R.L. and T.S. designed the research project. R.L. and J.B. supervised research. T.S. developed
681 and tested TEPID. J.C. performed PCR validations of TE variants. T.S. and S.R.E. performed
682 bioinformatic analysis. R.L., T.S., J.B. and S.R.E. prepared the manuscript.
683

684 ## COMPETING FINANCIAL INTERESTS

685 The authors declare no competing financial interests.

686 # REFERENCES

687 Aranzana MJ, Kim S, Zhao K, Bakker E, Horton M, Jakob K, Lister C, Molitor J, Shindo C, Tang
688 C, et al. 2005. Genome-Wide Association Mapping in Arabidopsis Identifies Previously
689 Known Flowering Time and Pathogen Resistance Genes. *PLoS Genetics* **1**: e60–9.

690 Bartenhagen C, Dugas M. 2013. RSVSim: an R/Bioconductor package for the simulation of
691 structural variations. *Bioinformatics* **29**: 1679–1681.

692 Bingham PM, Kidwell MG, Rubin GM. 1982. The molecular basis of P-M hybrid dysgenesis: the
693 role of the P element, a P-strain-specific transposon family. *Cell* **29**: 995–1004.

694 Blumenstiel JP, Hartl DL. 2005. Evidence for maternally transmitted small interfering RNA in the
695 repression of transposition in Drosophila virilis. *Proc Natl Acad Sci USA* **102**: 15965–15970.

696 Bolger A, Scossa F, Bolger ME, Lanz C, Maumus F, Tohge T, Quesneville H, Alseekh S,
697 Sørensen I, Lichtenstein G, et al. 2014. The genome of the stress-tolerant wild tomato
698 species. *Nat Genet* **46**: 1034–1038.

699 Bundock P, Hooykaas P. 2005. An Arabidopsis hAT-like transposase is essential for plant
700 development. *Nature* **436**: 282–284.

701 Calarco JP, Borges F, Donoghue MTA, Van Ex F, Jullien PE, Lopes T, Gardner R, Berger F,
702 FeijO JA, Becker JD, et al. 2012. Reprogramming of DNA Methylation in Pollen Guides
703 Epigenetic Inheritance via Small RNA. *Cell* **151**: 194–205.

704 Camacho C, Coulouris G, Avagyan V, Ma N, Papadopoulos J, Bealer K, Madden TL. 2009.
705 BLAST+: architecture and applications. *BMC Bioinformatics* **10**: 421.

706 Cao J, Schneeberger K, Ossowski S, Günther T, Bender S, Fitz J, Koenig D, Lanz C, Stegle O,
707 Lippert C, et al. 2011. Whole-genome sequencing of multiple Arabidopsis thaliana
708 populations. *Nat Genet* **43**: 956–963.

709 Chin C-S, Alexander DH, Marks P, Klammer AA, Drake J, Heiner C, Clum A, Copeland A,
710 Huddleston J, Eichler EE, et al. 2013. Nonhybrid, finished microbial genome assemblies
711 from long-read SMRT sequencing data. *Nat Meth* **10**: 563–569.

712 Cock PJA, Antao T, Chang JT, Chapman BA, Cox CJ, Dalke A, Friedberg I, Hamelryck T, Kauff
713 F, Wilczynski B, et al. 2009. Biopython: freely available Python tools for computational
714 molecular biology and bioinformatics. *Bioinformatics* **25**: 1422–1423.

715 Cokus SJ, Feng S, Zhang X, Chen Z, Merriman B, Haudenschild CD, Pradhan S, Nelson SF,
716 Pellegrini M, Jacobsen SE. 2008. Shotgun bisulphite sequencing of the Arabidopsis
717 genome reveals DNA methylation patterning. *Nature* **452**: 215–219.

718 Dale RK, Pedersen BS, Quinlan AR. 2011. Pybedtools: a flexible Python library for manipulating
719 genomic datasets and annotations. *Bioinformatics* **27**: 3423–3424.

720 Edwards K, Johnstone C, Thompson C. 1991. A simple and rapid method for the preparation of
721 plant genomic DNA for PCR analysis. *Nucleic Acids Research* **19**: 1349.

722 Faust GG, Hall IM. 2014. SAMBLASTER: fast duplicate marking and structural variant read
723 extraction. *Bioinformatics* **30**: 2503–2505.

724 Faust GG, Hall IM. 2012. YAHA: fast and flexible long-read alignment with optimal breakpoint
725 detection. *Bioinformatics* **28**: 2417–2424.

726 Gehring M, Pignatta D, Erdmann RM, Bell GW, Scheer E. 2014. *Data from: Natural epigenetic*
727 *polymorphisms lead to intraspecific variation in Arabidopsis gene imprinting*. Dryad Digital
728 Repository.

729 Gendrel AV, Lippman Z, Yordan C, Colot V, Martienssen RA. 2002. Dependence of
730 heterochromatic histone H3 methylation patterns on the Arabidopsis gene DDM1. *Science*
731 **297**: 1871–1873.

732 Grob S, Schmid MW, Grossniklaus U. 2014. Hi-C Analysis in Arabidopsis Identifies the KNOT, a
733 Structure with Similarities to the flamenco Locus of Drosophila. *Molecular Cell* 1–16.

734 Hénaff E, Vives C, Desvoyes B, Chaurasia A, Payet J, Gutierrez C, Casacuberta JM. 2014.
735 Extensive amplification of the E2F transcription factor binding sites by transposons during
736 evolution of Brassica species. *The Plant Journal* **77**: 852–862.

737 Hénaff E, Zapata L, Casacuberta JM, Ossowski S. 2015. Jitterbug: somatic and germline
738 transposon insertion detection at single-nucleotide resolution. *BMC Genomics* **16**: 1–16.

739 Hirochika H, Okamoto H, Kakutani T. 2000. Silencing of retrotransposons in Arabidopsis and
740 reactivation by the ddm1 mutation. *The Plant Cell* **12**: 357–369.

741 Hsieh TF, Ibarra CA, Silva P, Zemach A, Eshed-Williams L, Fischer RL, Zilberman D. 2009.
742 Genome-Wide Demethylation of Arabidopsis Endosperm. *Science* **324**: 1451–1454.

743 Ibarra CA, Feng X, Schoft VK, Hsieh T-F, Uzawa R, Rodrigues JA, Zemach A, Chumak N,
744 Machlicova A, Nishimura T, et al. 2012. Active DNA demethylation in plant companion cells
745 reinforces transposon methylation in gametes. *Science* **337**: 1360–1364.

746 Ito H, Gaubert H, Bucher E, Mirouze M, Vaillant I, Paszkowski J. 2011. Supplement An siRNA
747 pathway prevents transgenerational retrotransposition in plants subjected to stress -
748 supplement. *Nature* **472**: 115–119.

749 Jeddeloh JA, Stokes TL, Richards EJ. 1999. Maintenance of genomic methylation requires a
750 SWI2/SNF2-like protein. *Nat Genet* **22**: 94–97.

751 Jiang C, Mithani A, Belfield EJ, Mott R, Hurst LD, Harberd NP. 2014. Environmentally
752 responsive genome-wide accumulation of de novo Arabidopsis thaliana mutations and
753 epimutations. *Genome Research* **24**: 1821–1829.

754 Josefsson C, Dilkes B, Comai L. 2006. Parent-dependent loss of gene silencing during
755 interspecies hybridization. *Current Biology* **16**: 1322–1328.

756 Jullien PE, Susaki D, Yelagandula R, Higashiyama T, Berger F. 2012. DNA Methylation
757 Dynamics during Sexual Reproduction in Arabidopsis thaliana. *Curr Biol* **22**: 1825–1830.

758 Katoh A, Uenohara K, Akita M, Hashimoto T. 2006. Early steps in the biosynthesis of NAD in
759 Arabidopsis start with aspartate and occur in the plastid. *Plant Physiology* **141**: 851–857.

760 Kawashima T, Berger F. 2014. Epigenetic reprogramming in plantsexual reproduction. *Nature*
761 *Reviews Genetics* **15**: 613–624.

762 Langmead B, Salzberg SL. 2012. Fast gapped-read alignment with Bowtie 2. *Nat Meth* **9**: 357–
763 359.

764 Layer RM, Chiang C, Quinlan AR, Hall IM. 2014. LUMPY: a probabilistic framework for
765 structural variant discovery. *Genome Biology* **15**: R84.

766 Li H, Handsaker B, Wysoker A, Fennell T, Ruan J, Homer N, Marth G, Abecasis G, Durbin R,
767 1000 Genome Project Data Processing Subgroup. 2009. The Sequence Alignment/Map
768 format and SAMtools. *Bioinformatics* **25**: 2078–2079.

769 Lippman Z, Gendrel A-V, Black M, Vaughn MW, Dedhia N, McCombie WR, Lavine K, Mittal V,
770 May B, Kasschau KD, et al. 2004. Role of transposable elements in heterochromatin and
771 epigenetic control. *Nature* **430**: 471–476.

772 Lister R, O'Malley RC, Tonti-Filippini J, Gregory BD, Berry CC, Millar AH, Ecker JR. 2008.
773 Highly integrated single-base resolution maps of the epigenome in Arabidopsis. *Cell* **133**:
774 523–536.

775 Makarevitch I, Waters AJ, West PT, Stitzer M, Hirsch CN, Ross-Ibarra J, Springer NM. 2015.
776 Transposable Elements Contribute to Activation of Maize Genes in Response to Abiotic
777 Stress. *PLoS Genetics* **11**: e1004915.

778 Martienssen RA. 2010. Heterochromatin, small RNA and post-fertilization dysgenesis in
779 allopolyploid and interploid hybrids of Arabidopsis. *New Phytologist* **186**: 46–53.

780 Matzke MA, Mosher RA. 2014. RNA-directed DNA methylation: an epigenetic pathway of
781 increasing complexity. *Nature Reviews Genetics* **15**: 394–408.

782 Mirouze M, Reinders J, Bucher E, Nishimura T, Schneeberger K, Ossowski S, Cao J, Weigel D,
783 Paszkowski J, Mathieu O. 2009. Selective epigenetic control of retrotransposition in
784 Arabidopsis. *Nature* **461**: 427–430.

785 Miura A, Yonebayashi S, Watanabe K, Toyama T. 2001. Mobilization of transposons by a
786 mutation abolishing full DNA methylation in Arabidopsis. *Nature* **411**: 212–214.

787 Mosher RA, Melnyk CW, Kelly KA, Dunn RM, Studholme DJ, Baulcombe DC. 2009. Uniparental
788 expression of PolIV-dependent siRNAs in developing endosperm of Arabidopsis. *Nature*
789 **460**: 283–286.

790 Pignatta D, Erdmann RM, Scheer E, Picard CL, Bell GW, Gehring M. 2014. Natural epigenetic
791 polymorphisms lead to intraspecific variation in Arabidopsis gene imprinting. *eLife* **3**:
792 e03198.

793 Plasterk R. 1991. The Origin of Footprints of the Tc1 Transposon of Caenorhabditis elegans.

794 *EMBO* **10**: 1919–1925.

795 Quinlan AR, Hall IM. 2010. BEDTools: a flexible suite of utilities for comparing genomic
796 features. *Bioinformatics* **26**: 841–842.

797 Richards EJ. 2006. Inherited epigenetic variation - revisiting soft inheritance. *Nature Reviews*
798 *Genetics* **7**: 395–U2.

799 Robb S, Lu L, Valencia E, Burnette JM. 2013. The use of RelocaTE and unassembled short
800 reads to produce high-resolution snapshots of transposable element generated diversity in
801 rice. *G3: Genes*| *Genomes*| *Genetics*.

802 Saze H, Scheid OM, Paszkowski J. 2003. Maintenance of CpG methylation is essential for
803 epigenetic inheritance during plant gametogenesis. *Nat Genet* **34**: 65–69.

804 Schmitz RJ, Schultz MD, Urich MA, Nery JR, Pelizzola M, Libiger O, Alix A, McCosh RB, Chen
805 H, Schork NJ, et al. 2013. Patterns of population epigenomic diversity. *Nature* **495**: 193–
806 198.

807 Schneeberger K, Ossowski S, Ott F, Klein JD, Wang X, Lanz C, Smith LM, Cao J, Fitz J,
808 Warthmann N, et al. 2011. Reference-guided assembly of four diverse Arabidopsis thaliana
809 genomes. *Proc Natl Acad Sci USA* **108**: 10249–10254.

810 Slotkin RK, Vaughn M, Borges F, TanurdZiC M, Becker JD, FeijO JA, Martienssen RA. 2009.
811 Epigenetic reprogramming and small RNA silencing of transposable elements in pollen. *Cell*
812 **136**: 461–472.

813 Storey JD, Tibshirani R. 2003. Statistical significance for genomewide studies. *Proc Natl Acad*
814 *Sci USA* **100**: 9440–9445.

815 Stroud H, Greenberg MVC, Feng S, Bernatavichute YV, Jacobsen SE. 2013. Comprehensive
816 analysis of silencing mutants reveals complex regulation of the Arabidopsis methylome. *Cell*
817 **152**: 352–364.

818 Sullivan AM, Arsovski AA, Lempe J, Bubb KL, Weirauch MT, Sabo PJ, Sandstrom R, Thurman
819 RE, Neph S, Reynolds AP, et al. 2014. Mapping and dynamics of regulatory DNA and
820 transcription factor networks in A. thaliana. *Cell* **8**: 2015–2030.

821 Thung DT, de Ligt J, Vissers LE, Steehouwer M, Kroon M, de Vries P, Slagboom EP, Ye K,
822 Veltman JA, Hehir-Kwa JY. 2014. Mobster: accurate detection of mobile element insertions
823 in next generation sequencing data. 1–11.

824 Vitte C, Fustier M-A, Alix K, Tenaillon MI. 2014. The bright side of transposons in crop evolution.
825 *Briefings in Functional Genomics* **13**: 276–295.

826 Wang G, Ellendorff U, Kemp B, Mansfield JW, Forsyth A, Mitchell K, Bastas K, Liu C-M, Woods-
827 Tör A, Zipfel C, et al. 2008. A genome-wide functional investigation into the roles of
828 receptor-like proteins in Arabidopsis. *Plant Physiology* **147**: 503–517.

829 Wicker T, Sabot F, Hua-Van A, Bennetzen JL, Capy P, Chalhoub B, Flavell A, Leroy P,

830 Morgante M, Panaud O, et al. 2007. A unified classification system for eukaryotic
831 transposable elements. *Nature Reviews Genetics* **8**: 973–982.

832 Zemach A, Kim MY, Hsieh P-H, Coleman-Derr D, Eshed-Williams L, Thao K, Harmer SL,
833 Zilberman D. 2013. The Arabidopsis Nucleosome Remodeler DDM1 Allows DNA
834 Methyltransferases to Access H1-Containing Heterochromatin. *Cell* **153**: 193–205.

835 Zhang X, Yazaki J, Sundaresan A, Cokus S, Chan SWL, Chen H, Henderson IR, Shinn P,
836 Pellegrini M, Jacobsen SE, et al. 2006. Genome-wide High-Resolution Mapping and
837 Functional Analysis of DNA Methylation in Arabidopsis. *Cell* **126**: 1189–1201.

838 Zilberman D, Gehring M, Tran RK, Ballinger T, Henikoff S. 2007. Genome-wide analysis of
839 Arabidopsis thaliana DNA methylation uncovers an interdependence between methylation
840 and transcription. *Nat Genet* **39**: 61–69.

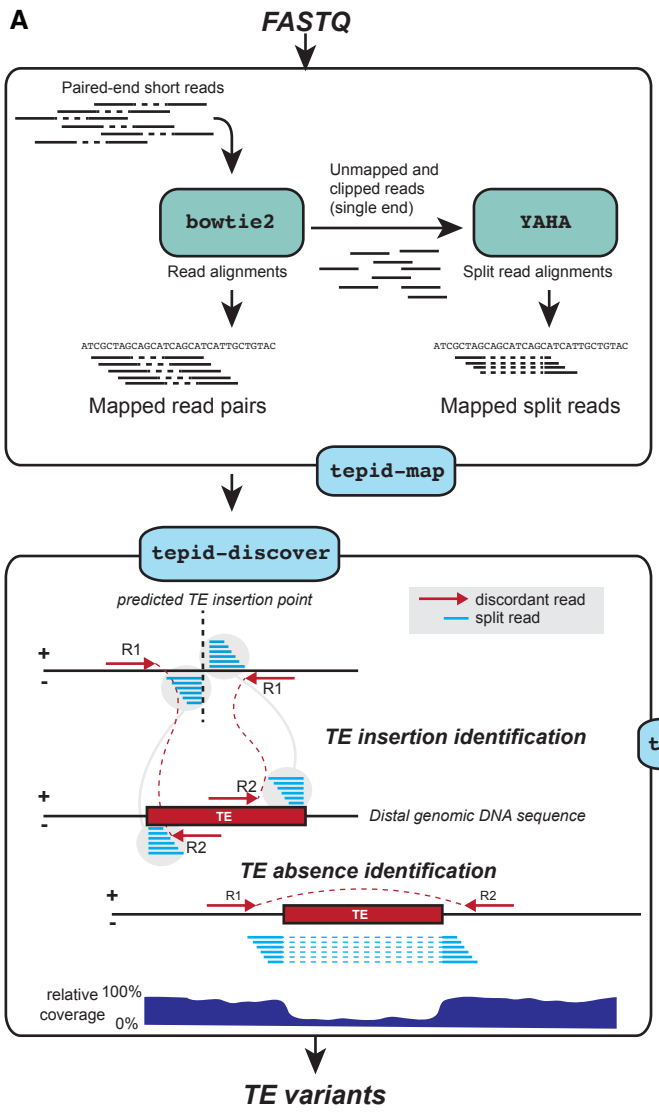

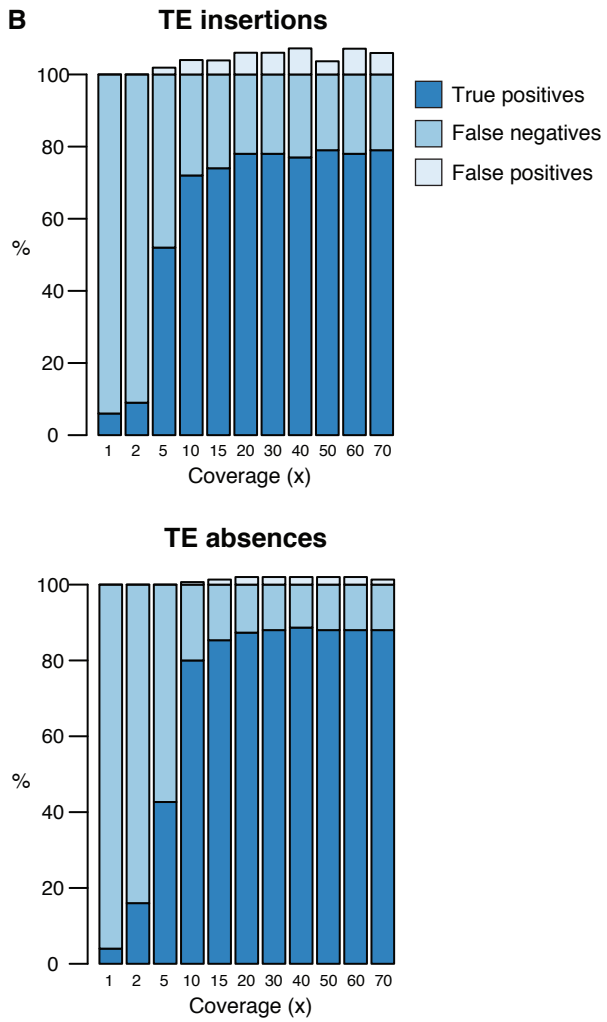

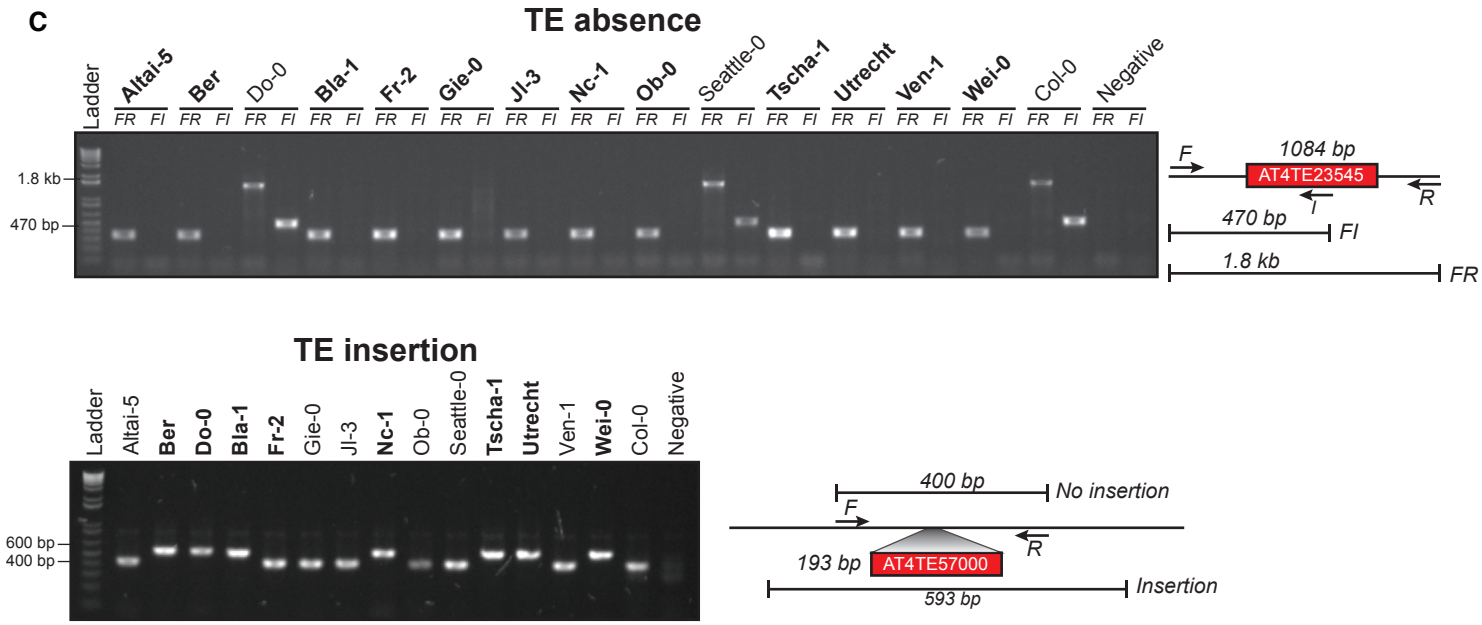

D

	True positives	False positives	False negatives
Absences	77.10%	9.16%	13.74%
Insertions	70.71%	9.29%	20.00%

842 **Figure 1. Design and testing of the TE variant discovery pipeline**

843 (A) Principle of TE variant discovery using split and discordant read mapping positions. Paired
844 end reads are first mapped to the reference genome using Bowtie2 (Langmead and Salzberg
845 2012). Soft-clipped or unmapped reads are then extracted from the alignment and re-mapped
846 using Yaha, a split read mapper (Faust and Hall 2012). All read alignments are then used by
847 TEPID to discover TE variants relative to the reference genome, in the 'tepid-discover' step.
848 When analyzing groups of related samples, these variants can be further refined using the
849 'tepid-refine' step, which examines in more detail the genomic regions where there was a TE
850 variant identified in another sample, and calls the same variant for the sample in question using
851 lower read count thresholds as compared to the 'tepid-discover' step, in order to reduce false
852 negative variant calls within a group of related samples.

853 (B) Testing of the TEPID pipeline using simulated TE variants in the Arabidopsis Col-0 genome
854 (TAIR10), for a range of sequencing coverage levels.

855 (C) PCR validation examples for TE presence/absence variant predictions. Accessions that
856 were predicted to contain a TE insertion or TE absence are marked in bold. For the example TE
857 absence variant, two primer sets were used; forward (F) and reverse (R) or internal (I).
858 Accessions with a TE absence will not produce the FI band and produce a shorter FR product,
859 with the change in size matching the size of the deleted TE. For the example TE insertion, one
860 primer set was used, spanning the TE insertion site. A band shift of approximately 200 bp can
861 be seen, corresponding to the size of the inserted TE.

862 (D) Summary table of PCR validation results for TE variants.

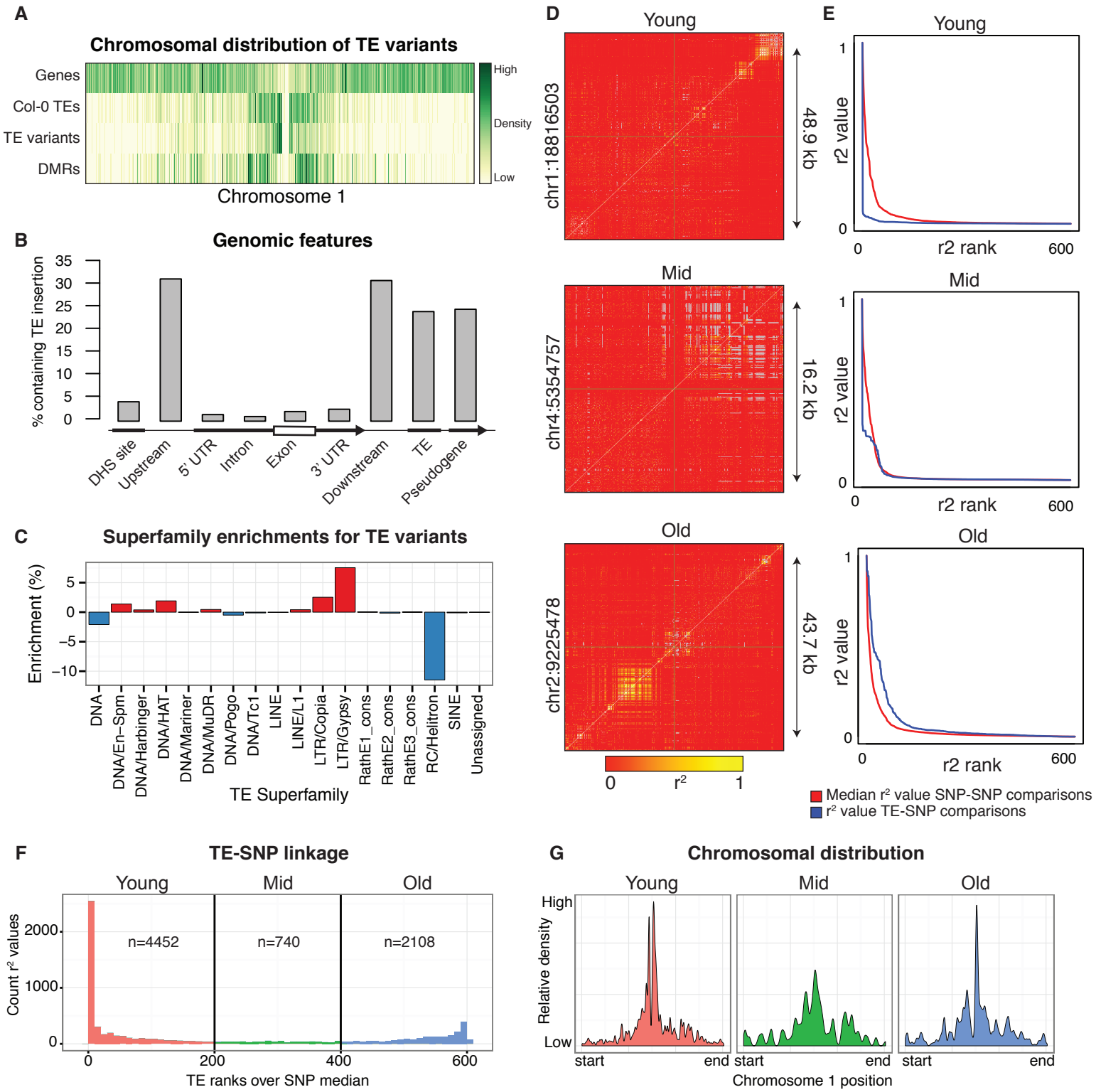
A
Chromosomal distribution of TE variants
Genes
Col-0 TEs
TE variants
DMRs
High
Density
Low
Chromosome 1
B
Genomic features
% containing TE insertion
35
30
25
20
15
10
5
0
DHS site
Upstream
5' UTR
Intron
Exon
3' UTR
Downstream
TE
Pseudogene
C
Superfamily enrichments for TE variants
Enrichment (%)
5
0
−5
−10
DNA
DNA/En−Spm
DNA/Harbinger
DNA/HAT
DNA/Mariner
DNA/MuDR
DNA/Pogo
DNA/Tc1
LINE
LINE/L1
LTR/Copia
LTR/Gypsy
RathE1_cons
RathE2_cons
RathE3_cons
RC/Helitron
SINE
Unassigned
TE Superfamily
D
Young
chr1:18816503
48.9 kb
Mid
chr4:5354757
16.2 kb
Old
chr2:9225478
43.7 kb
0
r²
1
E
Young
Mid
Old
r2 value
r2 rank
0
600
1
Median r² value SNP-SNP comparisons
r² value TE-SNP comparisons
F
TE-SNP linkage
Young
Mid
Old
Count r² values
2000
1000
0
n=4452
n=740
n=2108
0
200
400
600
TE ranks over SNP median
G
Chromosomal distribution
Young
Mid
Old
High
Relative density
Low
start
end
Chromosome 1 position

Figure 2. Extensive novel genetic diversity uncovered by TE variant analysis

(A) Distribution of identified TE variants on chromosome 1, with distributions of all Col-0 genes, Col-0 TEs, and population DMRs.

(B) Frequency of TE variants at different genomic features.

(C) Enrichment and depletion of TE variants categorized by TE superfamily compared to the expected frequency due to genomic occurrence.

(D) r^2 correlation matrices for individual representative young, mid, and old TE variants.

(E) Rank order plots for individual representative young, mid, and old TE variants (matching those shown in D). Red line indicates the median r^2 value for each rank across SNP-based values. Blue line indicates r^2 values for TE-SNP comparisons.

(F) Histogram of the number of TE r^2 ranks (0-600) that are above the SNP-based median r^2 value for testable TE variants. TE variants with <200 ranks over the SNP median were classified as “young” elements, as they are not yet linked to the surrounding SNPs. TE variants with 200-400 ranks over the SNP median were classified as “mid” aged. TE variants with >400 ranks over the SNP median were classified as “old” elements, as they were linked to the surrounding SNPs.

(G) Chromosomal distribution of TE variants by age.

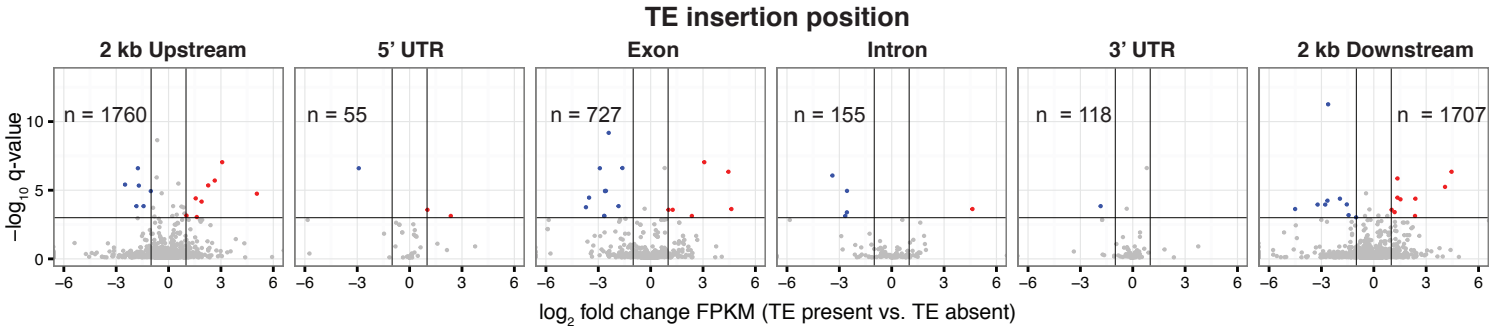
TE insertion position
2 kb Upstream
5' UTR
Exon
Intron
3' UTR
2 kb Downstream
n = 1760
n = 55
n = 727
n = 155
n = 118
n = 1707
−log10 q-value
log2 fold change FPKM (TE present vs. TE absent)

882 **Figure 3. Differential transcript abundance associated with genic TE variant**
883 **presence/absence**

884 Volcano plots showing transcript abundance differences for genes associated with TE insertion
885 variants at different positions, indicated in the plot titles. Genes with significantly different
886 transcript abundance in accessions with a TE insertion compared to accessions without a TE
887 insertion are colored blue (lower transcript abundance in accessions containing TE insertion) or
888 red (higher transcript abundance in accessions containing TE insertion). Vertical lines indicate
889 ±2 fold change in FPKM.

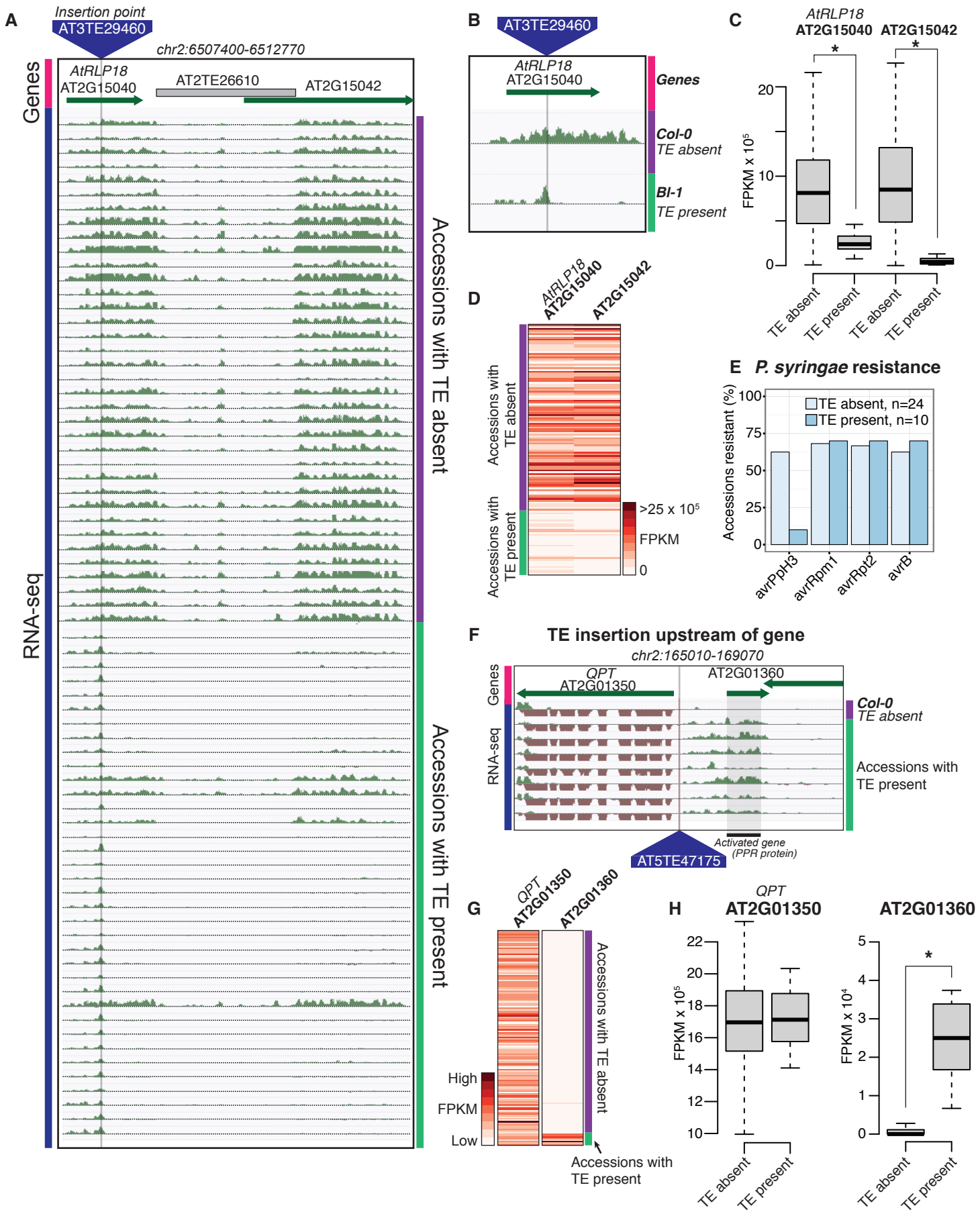
A
Insertion point
AT3TE29460
chr2:6507400-6512770
Genes
AtRLP18
AT2G15040
AT2TE26610
AT2G15042
RNA-seq
Accessions with TE absent
Accessions with TE present
B
AT3TE29460
AtRLP18
AT2G15040
Genes
Col-0
TE absent
Bl-1
TE present
C
AtRLP18
AT2G15040
AT2G15042
FPKM x 10^5
TE absent
TE present
TE absent
TE present
D
AtRLP18
AT2G15040
AT2G15042
Accessions with TE absent
Accessions with TE present
>25 x 10^5
FPKM
0
E
P. syringae resistance
Accessions resistant (%)
TE absent, n=24
TE present, n=10
avrPpH3
avrRpm1
avrRpt2
avrB
F
TE insertion upstream of gene
chr2:165010-169070
Genes
RNA-seq
QPT
AT2G01350
AT2G01360
Col-0
TE absent
Accessions with TE present
AT5TE47175
Activated gene
(PPR protein)
G
QPT
AT2G01350
AT2G01360
High
FPKM
Low
Accessions with TE absent
Accessions with TE present
H
QPT
AT2G01350
AT2G01360
FPKM x 10^5
FPKM x 10^4
TE absent
TE present
TE absent
TE present

891 **Figure 4. Effects of TE variants on local gene expression**

892 (A) Genome browser representation of RNA-seq data for genes *AtRLP18* (AT2G15040) and a
893 leucine-rich repeat family protein (AT2G15042) for all accessions containing a TE insertion
894 within the exon of the gene *AtRLP18*, and for a random subset of accessions not containing the
895 TE insertion within the exon of *AtRLP18*.

896 (B) Magnified view of the TE insertion variant within the *AtRLP18* exon.

897 (C) Boxplots comparing transcript abundance of *AtRLP18* and AT2G15042 in accessions with
898 and without the TE insertion in the *AtRLP18* exon. Asterisk indicates statistical significance ($p <$
899 5.8×10^{-10}; Mann-Whitney U test). Boxes represent the interquartile range (IQR) from quartile 1
900 to quartile 3. Boxplot upper whiskers represent the maximum value, or the upper value of the
901 quartile 3 plus 1.5 times the IQR (whichever is smaller). Boxplot lower whisker represents the
902 minimum value, or the lower value of the quartile 1 minus 1.5 times the IQR (whichever is
903 larger).

904 (D) Heatmap showing *AtRLP18* and AT2G15042 RNA-seq FPKM values for all accessions.

905 (E) Percentage of accessions with resistance to *Pseudomonas syringae* transformed with
906 different *avr* genes, for accessions containing or not containing a TE insertion in *AtRLP18.*

907 (F) Genome browser representation of RNA-seq data for a PPR protein-encoding gene
908 (AT2G01360) and *QPT* (AT2G01350), showing transcript abundance for these genes in
909 accessions containing a TE insertion variant in the upstream region of these genes.

910 (G) Heatmap representation of RNA-seq FPKM values for *QPT* and a gene encoding a PPR
911 protein (AT2G01360), for all accessions. Note that scales are different for the two heatmaps,
912 due to the higher transcript abundance of *QPT* compared to AT2G01360. Scale maximum for
913 AT2G01350 is 3.1×10^{5}, and for AT2G01360 is 5.9×10^{4}.

914 (H) Boxplots showing RNA-seq FPKM differences for *QPT* and AT2G01360 associated with

915 presence/absence of a TE variant in the gene upstream region. Asterisk indicates statistical

916 significance ($p < 1.8 \times 10^{-7}$, Mann-Whitney U test). Boxplots were constructed as for C.

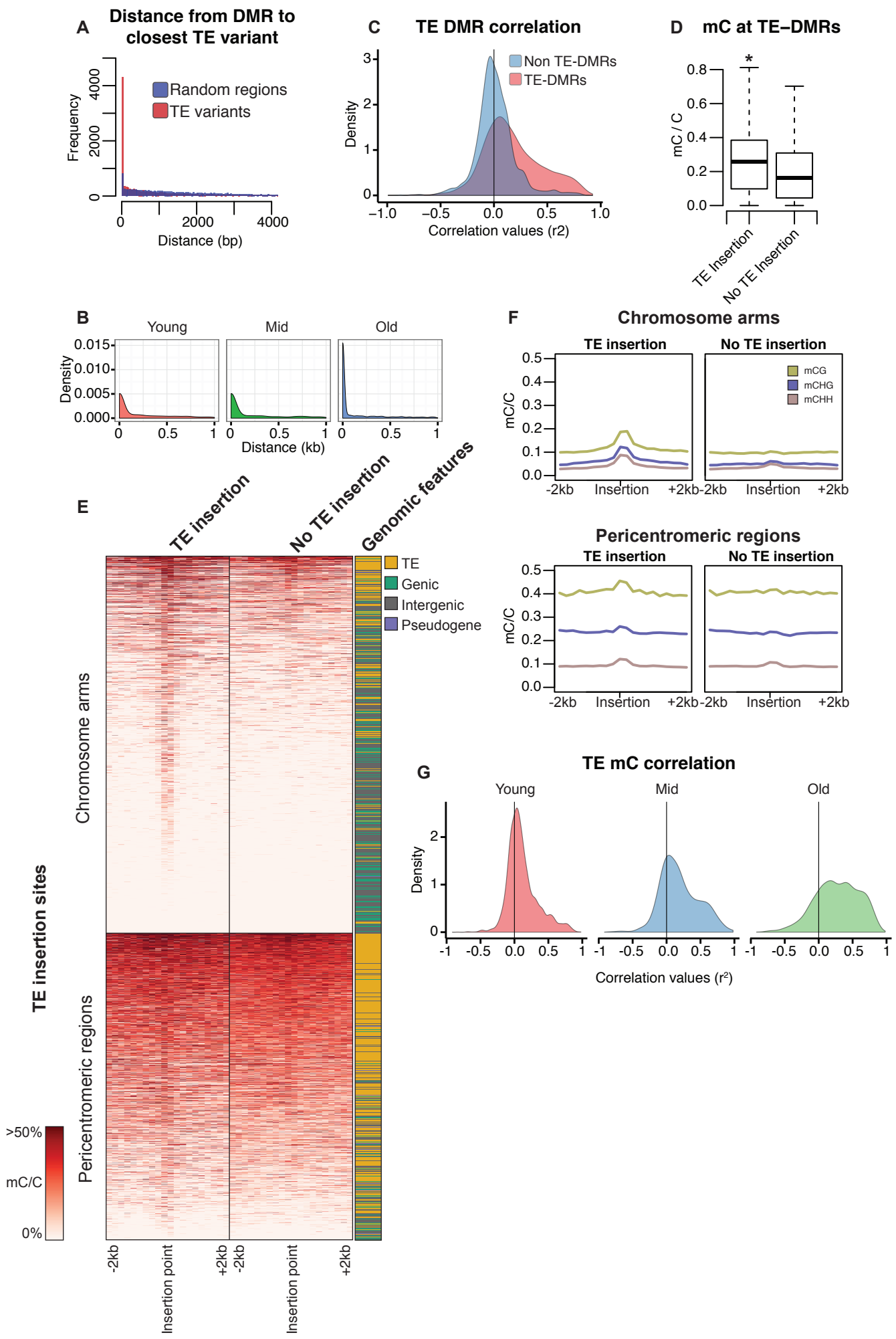
A
Distance from DMR to closest TE variant
Random regions
TE variants
Frequency
Distance (bp)
C
TE DMR correlation
Non TE-DMRs
TE-DMRs
Density
Correlation values (r2)
D
mC at TE–DMRs
mC / C
TE Insertion
No TE Insertion
B
Young
Mid
Old
Density
Distance (kb)
F
Chromosome arms
TE insertion
No TE insertion
mC/C
mCG
mCHG
mCHH
-2kb
Insertion
+2kb
Pericentromeric regions
E
TE insertion
No TE insertion
Genomic features
TE
Genic
Intergenic
Pseudogene
Chromosome arms
Pericentromeric regions
TE insertion sites
>50%
mC/C
0%
Insertion point
G
TE mC correlation
Young
Mid
Old
Density
Correlation values (r²)

918 **Figure 5. TE variants are associated with DNA methylation changes**

919 (A) Distance from each population DMR to closest TE variant (red), compared with a set of
920 randomly selected regions of the genome, of the same size as all TE variants (blue).

921 (B) Density of distance measurements between population DMRs and the closest TE variant,
922 grouped by age classification of TE variant.

923 (C) Density of Pearson correlation values between DNA methylation levels at population DMRs
924 and the presence/absence of the nearest TE variants. Pearson correlation values for population
925 DMRs within 1 kb of a TE variant (TE-DMRs) are shown in red, while values for population
926 DMRs further than 1 kb from a TE variant (non TE-DMRs) are shown in blue.

927 (D) Boxplot showing DNA methylation levels at TE-DMRs for accessions containing the TE
928 insertion and accessions not containing the TE insertion. Asterisk indicates statistical
929 significance ($p < 2.2 \times 10^{-16}$, Welch's t-test). Boxplots were constructed as for Figure 4C.

930 (E) DNA methylation levels in 200 bp windows ± 2 kb from TE insertion sites, for accessions
931 with and without the TE insertion. Heatmap is separated into in regions of the genome less than
932 3 Mb from a centromere (pericentromeric regions) or greater than 3 Mb from a centromere
933 (chromosome arms), and sorted by total DNA methylation at each locus.

934 (F) Average DNA methylation levels in mCG, mCHG and mCHH contexts in regions
935 surrounding TE insertion variant sites for pericentromeric insertions and insertions in the
936 euchromatic chromosome arms.

937 (G) Density of Pearson correlation values between DNA methylation levels in 200 bp regions
938 flanking TE variant sites and the presence/absence of the TE variant, separated by TE age
939 groups. Only TEs that were able to be assigned an age group are shown (total 7,300; minor
940 allele frequency >3%).

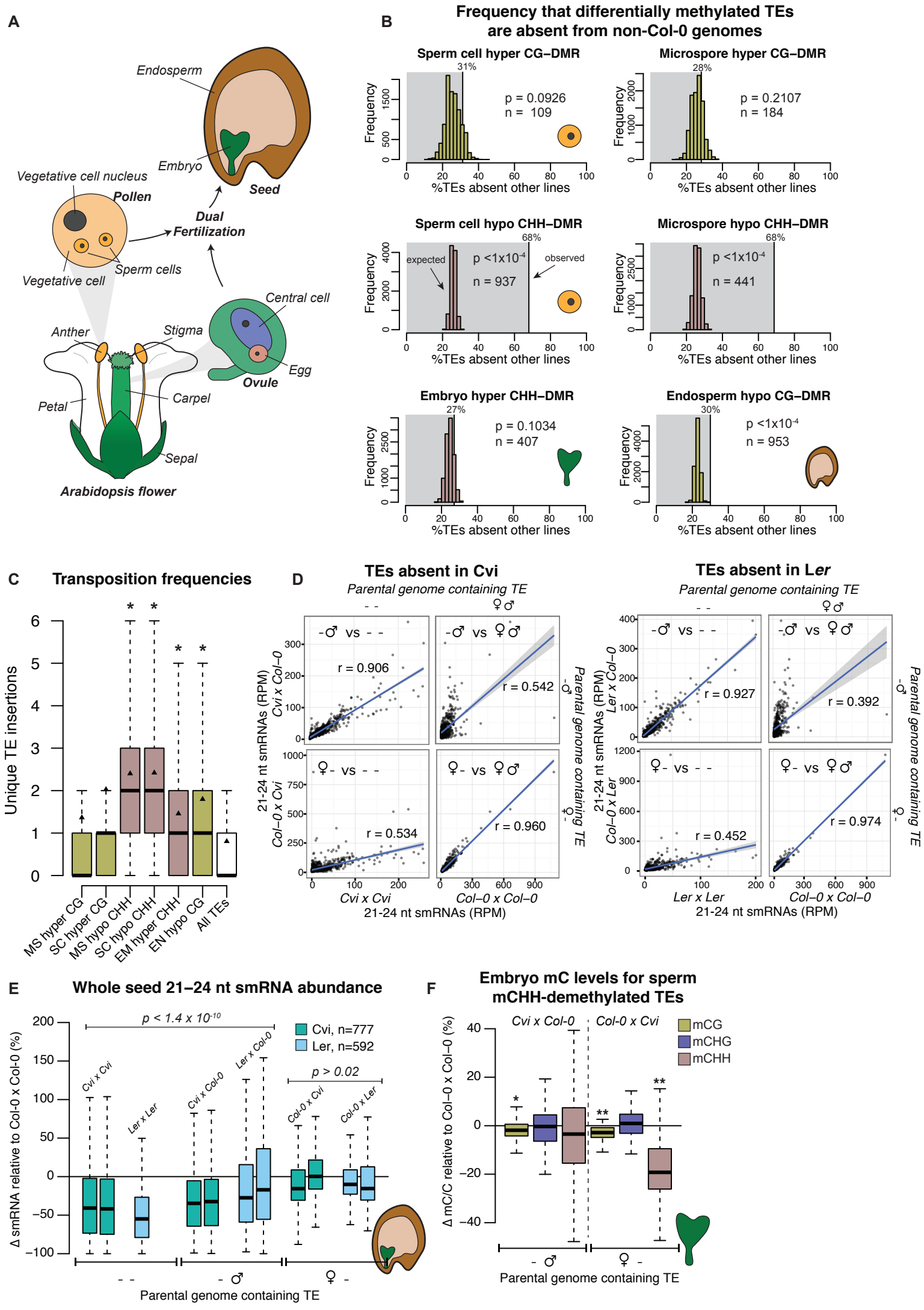
A
Endosperm
Embryo
Seed
Vegetative cell nucleus
Pollen
Dual Fertilization
Sperm cells
Vegetative cell
Central cell
Anther
Stigma
Egg
Ovule
Petal
Carpel
Sepal
Arabidopsis flower
B
Frequency that differentially methylated TEs are absent from non-Col-0 genomes
Sperm cell hyper CG–DMR
31%
p = 0.0926
n = 109
Microspore hyper CG–DMR
28%
p = 0.2107
n = 184
Sperm cell hypo CHH–DMR
68%
expected
observed
p <1x10-4
n = 937
Microspore hypo CHH–DMR
68%
p <1x10-4
n = 441
Embryo hyper CHH–DMR
27%
p = 0.1034
n = 407
Endosperm hypo CG–DMR
30%
p <1x10-4
n = 953
Frequency
%TEs absent other lines
C
Transposition frequencies
Unique TE insertions
MS hyper CG
SC hyper CG
MS hypo CHH
SC hypo CHH
EM hyper CHH
EN hypo CG
All TEs
D
TEs absent in Cvi
Parental genome containing TE
r = 0.906
r = 0.542
r = 0.534
r = 0.960
21-24 nt smRNAs (RPM)
Cvi x Cvi
Col–0 x Col–0
TEs absent in Ler
r = 0.927
r = 0.392
r = 0.452
r = 0.974
Ler x Ler
E
Whole seed 21–24 nt smRNA abundance
p < 1.4 x 10-10
Cvi, n=777
Ler, n=592
p > 0.02
Cvi x Cvi
Ler x Ler
Cvi x Col-0
Ler x Col-0
Col-0 x Cvi
Col-0 x Ler
Δ smRNA relative to Col-0 x Col-0 (%)
Parental genome containing TE
F
Embryo mC levels for sperm mCHH-demethylated TEs
Cvi x Col-0
Col-0 x Cvi
mCG
mCHG
mCHH
Δ mC/C relative to Col–0 x Col–0 (%)
Parental genome containing TE

942 **Figure 6. Genetic differences between parents is associated with demethylation of**
943 **transposable elements in hybrid progeny**
944 (A) Diagram of the developing pollen, ovule, and seed. During dual fertilization, one sperm
945 fertilizes the egg forming the embryo, while the other fertilizes the central cell to form the
946 endosperm.
947 (B) Percentage of TEs differentially methylated in germline cell types that were absent in at least
948 one non-Col-0 accession (shaded region) and expected percentage (histogram). 68% of TEs
949 that lose mCHH in the sperm cell or microspore are absent from non-reference accessions,
950 significantly more often than expected ($p < 1 \times 10^{-4}$, determined by resampling 10,000 times).
951 Embryo DMRs are in comparison to aerial tissues, endosperm DMRs are in comparison to the
952 embryo.
953 (C) Frequency of transposition for TEs differentially methylated in the microspore (MS), sperm
954 cell (SC), embryo (EM) and endosperm (EN). Black triangles represent the mean number of
955 unique TE insertion sites caused by elements in each list, asterisk indicates significance ($p < 1 \times$
956 10^{-5}, Welch's t-test). Boxplots were constructed as for Figure 4C.
957 (D) Correlation between whole seed 21-24 nt smRNA levels (normalized reads per million
958 values in 300 bp windows; RPM) for TEs present in maternal or paternal genomes only,
959 compared with smRNA levels in crosses where the TE is present or absent in both parental
960 genomes. Direction of each cross is represented on axes as *female x male*. TE variants are
961 always present in the Col-0 genome and absent in the non-Col-0 genome. R values are
962 Pearson's correlation coefficient.
963 (E) Whole seed 21-24 nt smRNA abundance (RPM, as for D) in TEs absent in Cvi for crosses
964 between Cvi and Col-0, or absent in L*er* for crosses between L*er* and Col-0. Direction of each
965 cross is represented as *female x male* on boxplot labels. Replicates are plotted side-by-side, p-

966 values are the result of a Mann-Whitney U test using averaged replicate data. Boxplots were
967 constructed as for Figure 4C.
968 (F) Embryonic DNA methylation levels 6 days after pollination for Cvi-absent TEs that lose
969 mCHH in sperm, following reciprocal crosses between Col-0 and Cvi. Boxplots were
970 constructed as for Figure 4C.

A

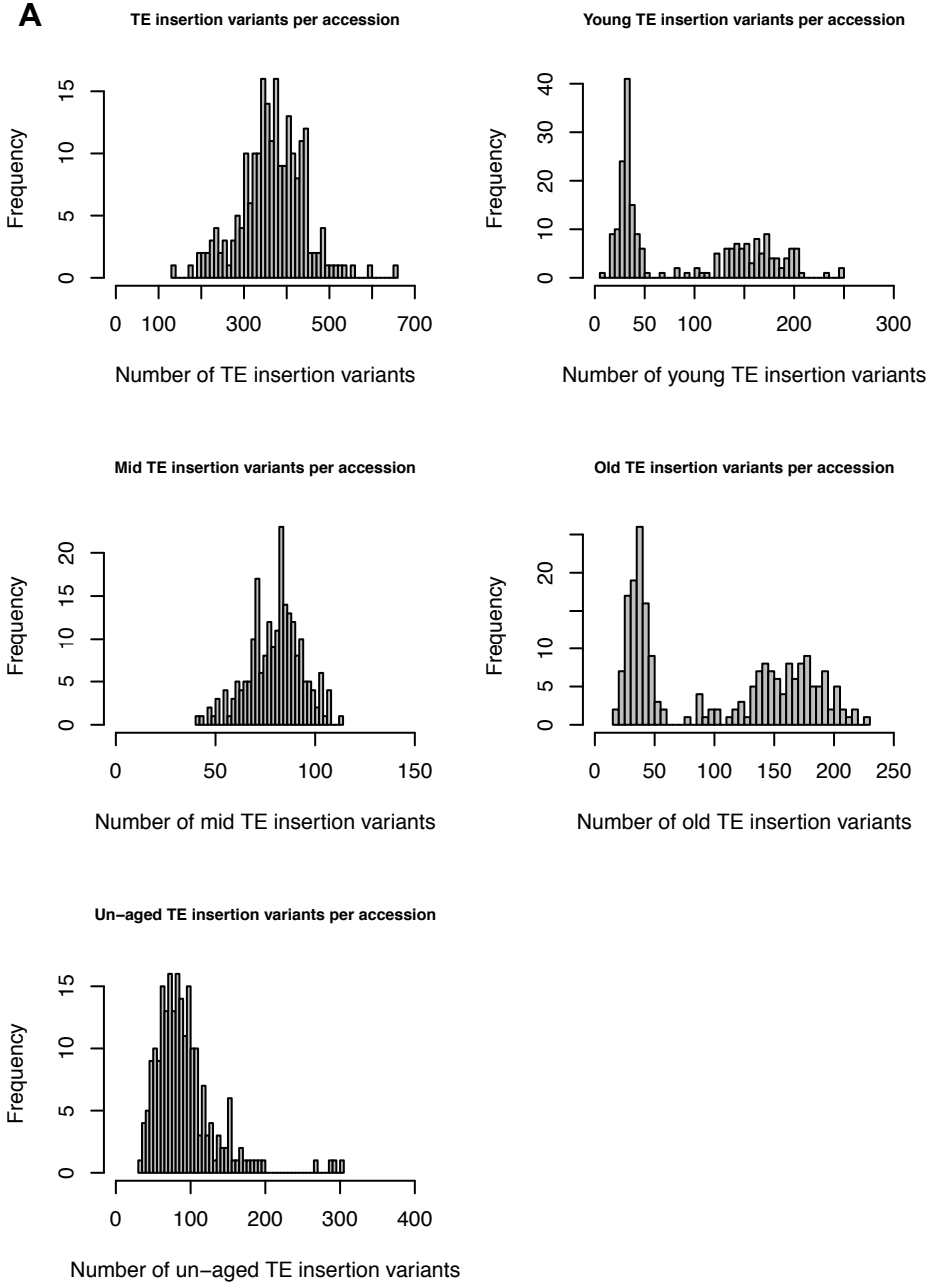
TE insertion variants per accession
Frequency
0
5
10
15
0
100
300
500
700
Number of TE insertion variants
Young TE insertion variants per accession
Frequency
0
10
20
30
40
0
50
100
200
300
Number of young TE insertion variants
Mid TE insertion variants per accession
Frequency
0
5
10
15
20
0
50
100
150
Number of mid TE insertion variants
Old TE insertion variants per accession
Frequency
0
5
10
20
0
50
100
150
200
250
Number of old TE insertion variants
Un−aged TE insertion variants per accession
Frequency
0
5
10
15
0
100
200
300
400
Number of un−aged TE insertion variants

B

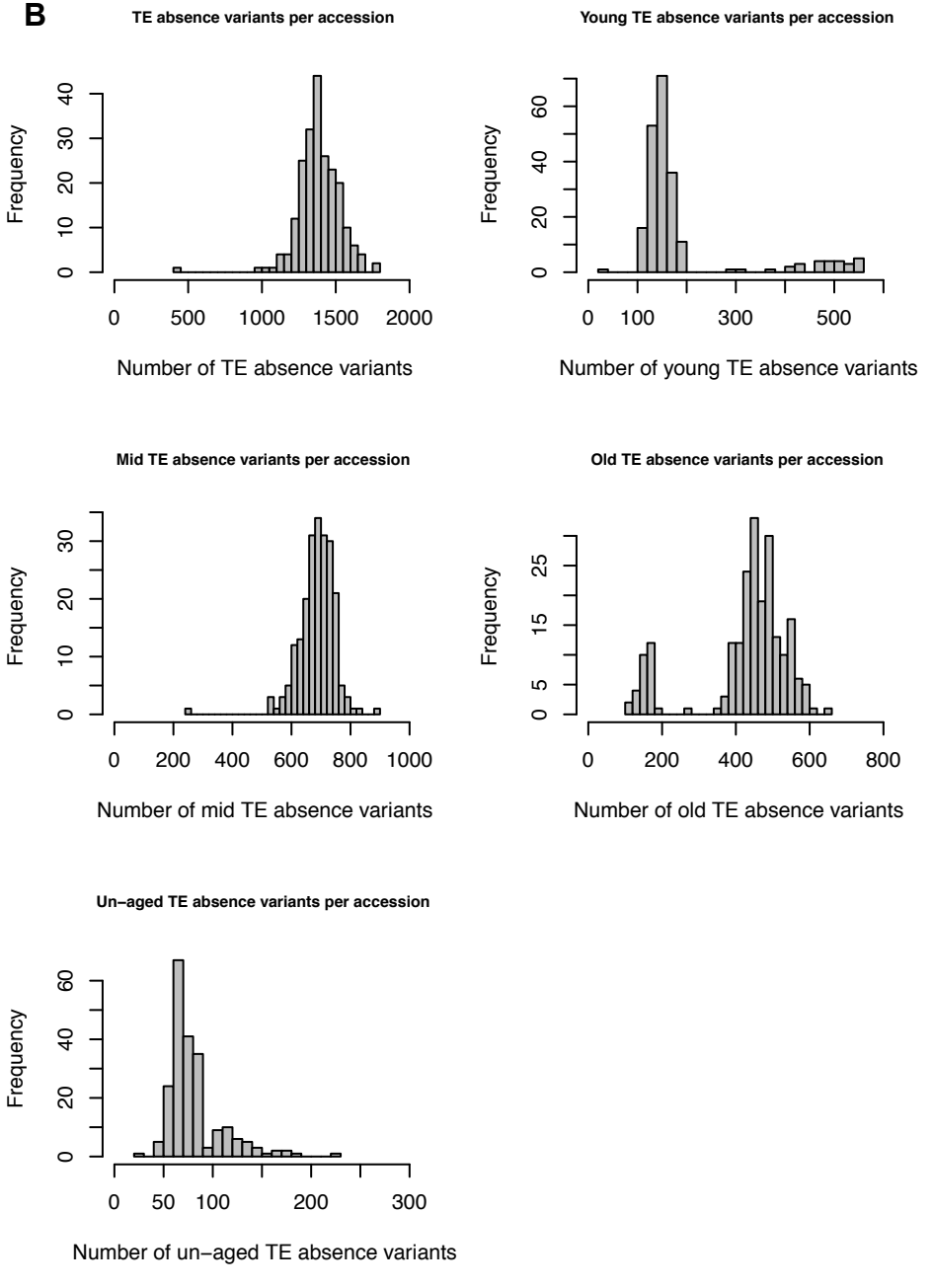
TE absence variants per accession
Frequency
0
10
20
30
40
0
500
1000
1500
2000
Number of TE absence variants
Young TE absence variants per accession
Frequency
0
20
40
60
0
100
300
500
Number of young TE absence variants
Mid TE absence variants per accession
Frequency
0
10
20
30
0
200
400
600
800
1000
Number of mid TE absence variants
Old TE absence variants per accession
Frequency
0
5
15
25
0
200
400
600
800
Number of old TE absence variants
Un−aged TE absence variants per accession
Frequency
0
20
40
60
0
50
100
200
300
Number of un−aged TE absence variants

Figure 2 - figure supplement 1. Number of TE presence/absence variants identified for each wild accession.

(A) Histograms showing number of TE insertion variants identified for each accession, separated by all TE insertions, and the different TE insertion age classes.

(B) TE absence variants as for A.

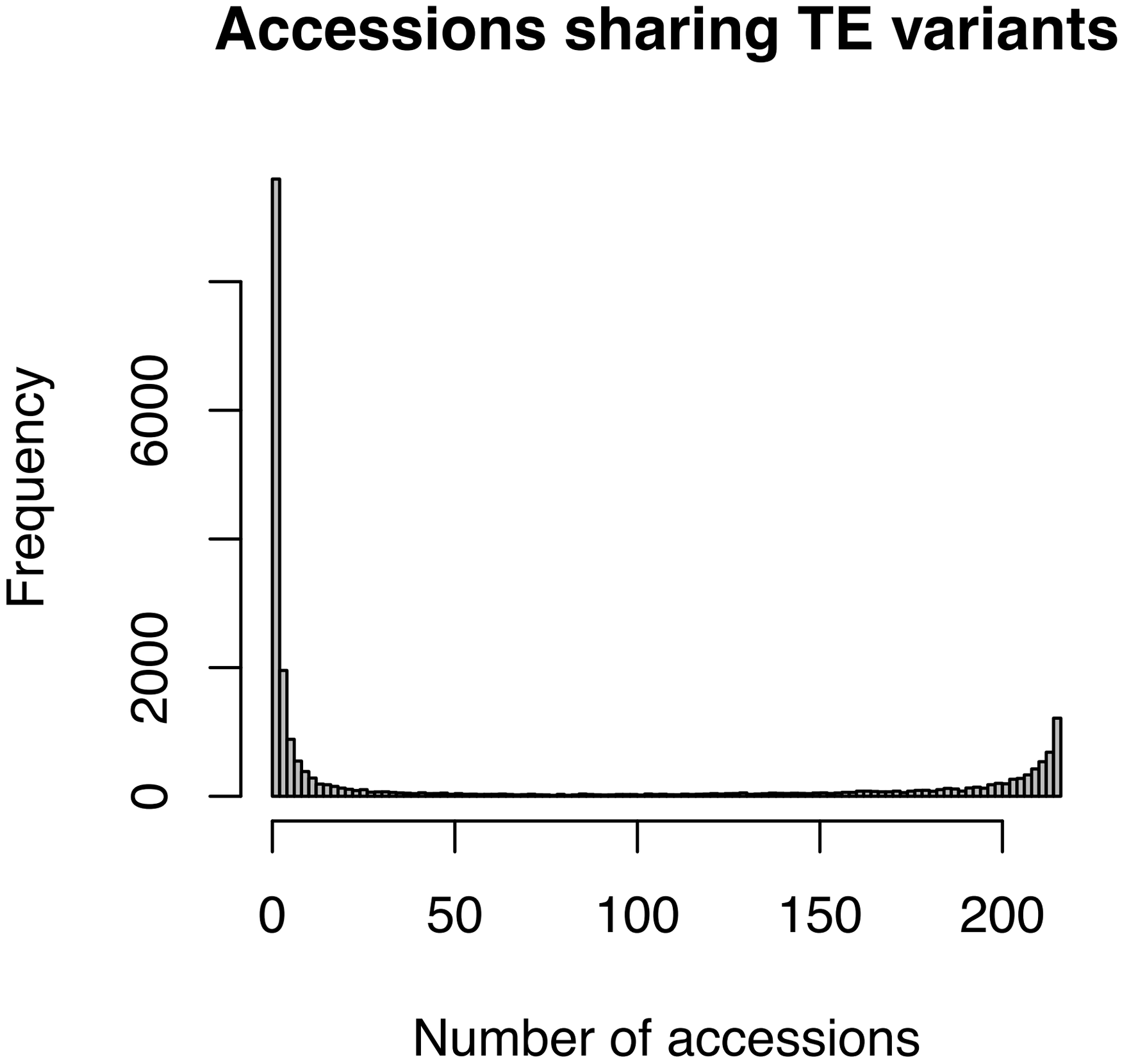
Accessions sharing TE variants
Frequency
0
2000
6000
0
50
100
150
200
Number of accessions

978 **Figure 2 - figure supplement 2. Histogram showing number of accessions sharing each**

979 **TE variant identified.**

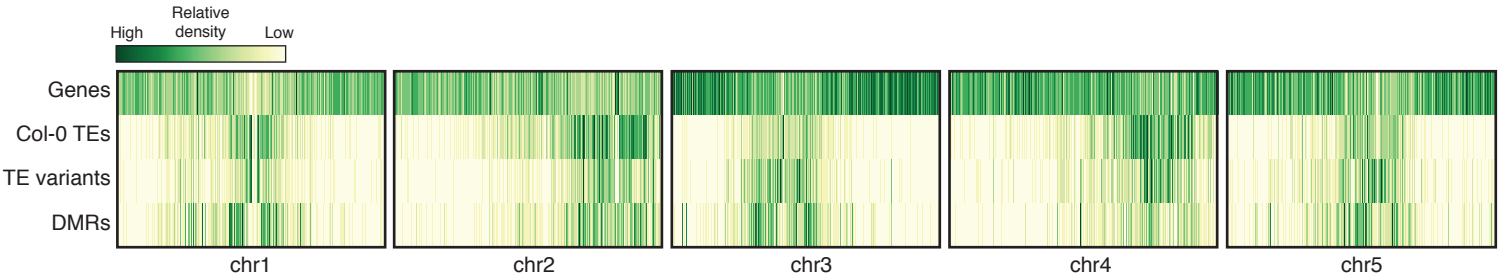
Relative density
High
Low
Genes
Col-0 TEs
TE variants
DMRs
chr1
chr2
chr3
chr4
chr5

981 **Figure 2 - figure supplement 3. Chromosomal distributions of genes, Col-0 TEs, TE**

982 **variants and population DMRs**

A

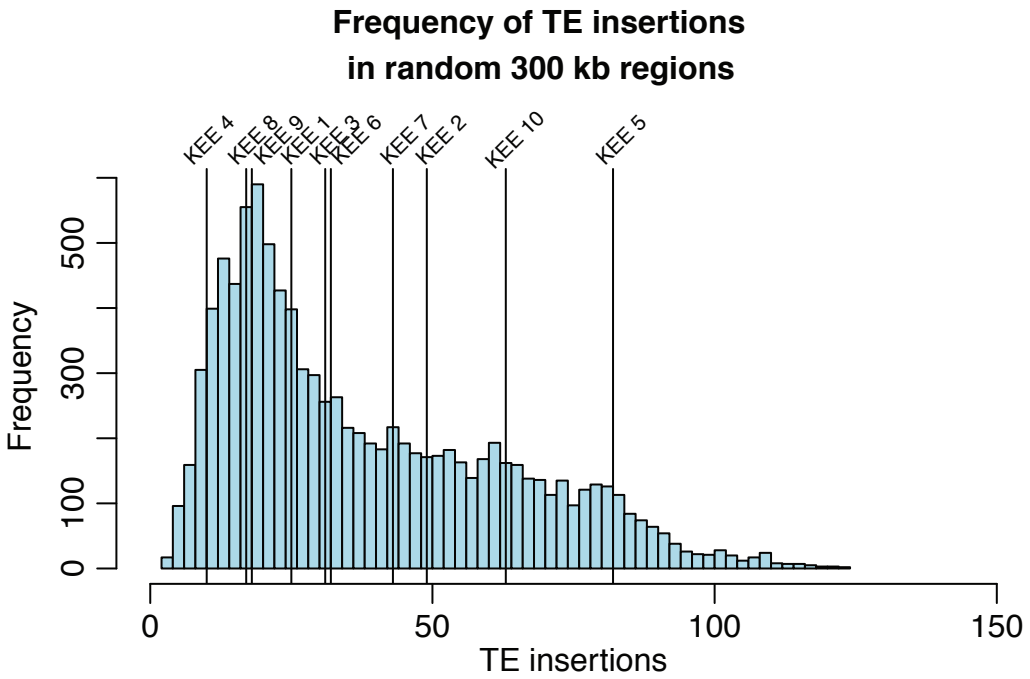

B

KEE	Chromosome	Start	Stop	TE insertions	p-value
kee1	chr1	6900000	7200000	25	0.585
kee2	chr2	4025000	4325000	49	0.306
kee3	chr3	1800000	2100000	31	0.4906
kee4	chr3	2950000	3250000	10	0.9424
kee5	chr3	16537500	16837500	82	0.0632
kee6	chr3	22375000	22675000	32	0.4785
kee7	chr4	10900000	11200000	43	0.3613
kee8	chr4	15387500	15687500	17	0.7863
kee9	chr5	4612500	4912500	18	0.7557
kee10	chr5	10162500	10462500	63	0.1857

984 **Figure 2 - figure supplement 4. Frequency of TE insertion variants in the *KNOT* region.**

985 (A) Number of TE insertion variants within each 300 kb *KNOT ENGAGED ELEMENT (KEE,*
986 vertical lines) and the number of TE insertion variants found in 10,000 randomly selected 300 kb
987 windows (histogram).

988 (B) Table showing number of TE insertion variants within each *KEE* region, and the associated
989 p-value determined by resampling 10,000 times.

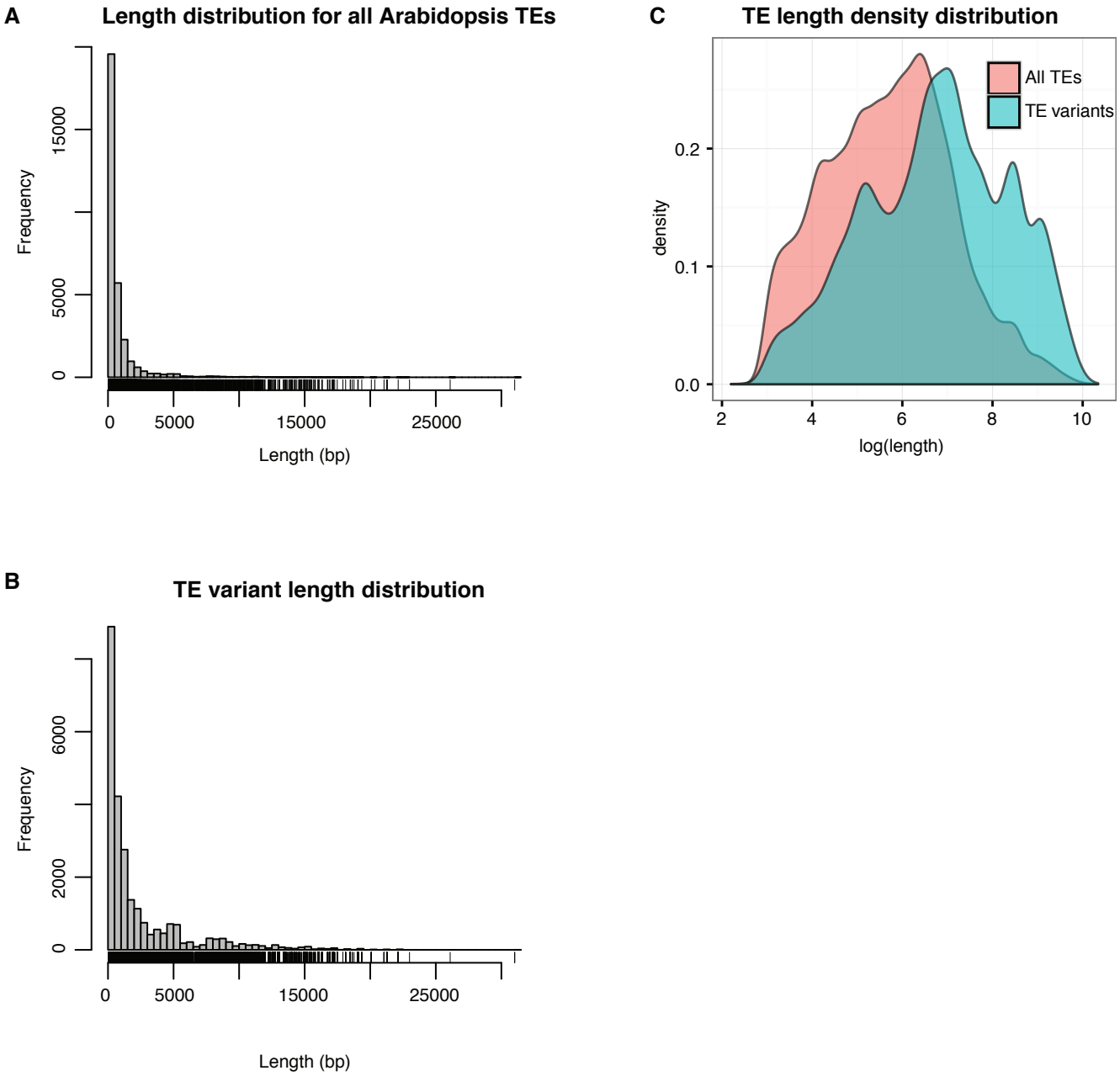
A
Length distribution for all Arabidopsis TEs
Frequency
0
5000
15000
0
5000
15000
25000
Length (bp)
C
TE length density distribution
All TEs
TE variants
density
0.0
0.1
0.2
2
4
6
8
10
log(length)
B
TE variant length distribution
Frequency
0
2000
6000
0
5000
15000
25000
Length (bp)

991 **Figure 2 - figure supplement 5. Length distributions for all Col-0 TEs and TE variants**

992 (A) Histogram showing lengths of all annotated TEs in the Col-0 reference genome.

993 (B) Histogram showing lengths of all TE variants.

994 (C) Density distribution of $\log_{10}$ TE length for all Col-0 TEs (red) and TE variants (blue).

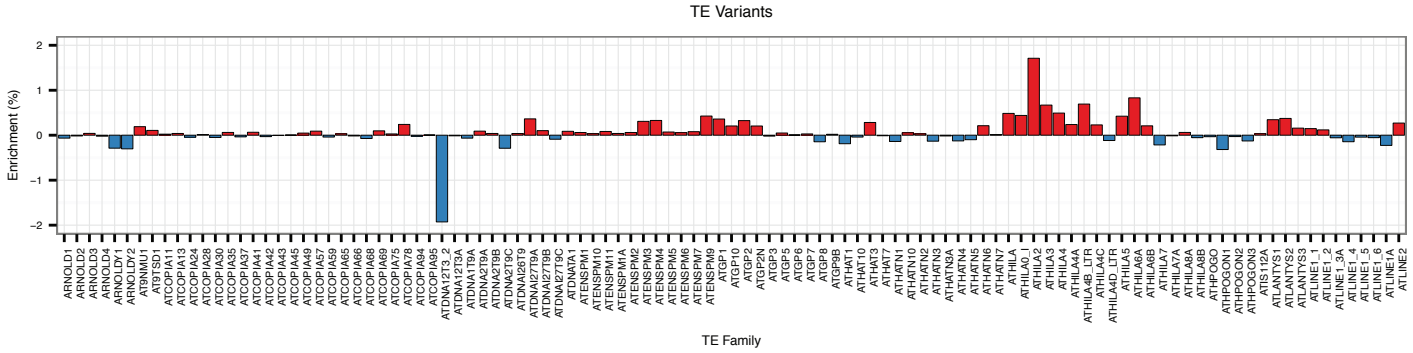
TE Variants
Enrichment (%)
2
1
0
−1
−2
ARNOLD1
ARNOLD2
ARNOLD3
ARNOLD4
ARNOLDY1
ARNOLDY2
AT9NMU1
AT9TSD1
ATCOPIA11
ATCOPIA13
ATCOPIA24
ATCOPIA28
ATCOPIA30
ATCOPIA35
ATCOPIA37
ATCOPIA41
ATCOPIA42
ATCOPIA43
ATCOPIA45
ATCOPIA49
ATCOPIA57
ATCOPIA59
ATCOPIA65
ATCOPIA66
ATCOPIA68
ATCOPIA69
ATCOPIA75
ATCOPIA78
ATCOPIA94
ATCOPIA95
ATDNA12T3_2
ATDNA12T3A
ATDNA1T9A
ATDNA2T9A
ATDNA2T9B
ATDNA2T9C
ATDNAI26T9
ATDNAI27T9A
ATDNAI27T9B
ATDNA27T9C
ATDNATA1
ATENSPM1
ATENSPM10
ATENSPM11
ATENSPM2
ATENSPM3
ATENSPM4
ATENSPM5
ATENSPM6
ATENSPM7
ATENSPM9
ATGP1
ATGP10
ATGP2
ATGP2N
ATGP3
ATGP5
ATGP6
ATGP7
ATGP8
ATGP9B
ATHAT1
ATHAT10
ATHAT13
ATHAT7
ATHATN1
ATHATN10
ATHATN2
ATHATN3
ATHATN3A
ATHATN4
ATHATN5
ATHATN6
ATHATN7
ATHILA
ATHILAO_I
ATHILA2
ATHILA3
ATHILA4
ATHILA4A
ATHILA4B_LTR
ATHILA4C
ATHILA4D_LTR
ATHILA5
ATHILA6A
ATHILA6B
ATHILA7
ATHILA7A
ATHILA8A
ATHILA8B
ATHPOGO
ATHPOGON1
ATHPOGON2
ATHPOGON3
ATIS112A
ATLANTYS1
ATLANTYS2
ATLANTYS3
ATLINE1_1
ATLINE1_2
ATLINE1_3A
ATLINE1_4
ATLINE1_5
ATLINE1_6
ATLINE1A
ATLINE2
TE Family

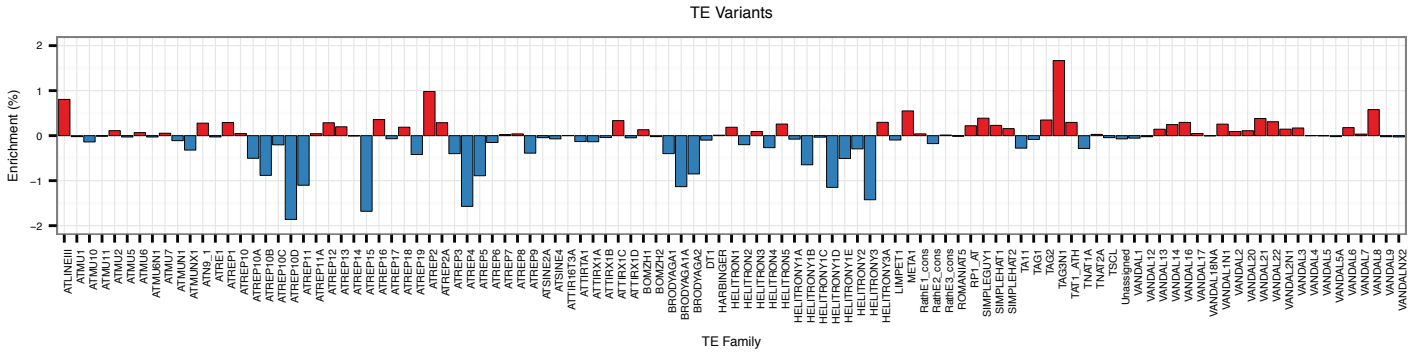
TE Variants
Enrichment (%)
2
1
0
−1
−2
ATLINEIII
ATMU1
ATMU10
ATMU11
ATMU5
ATMU6
ATMU6N1
ATMU7
ATMUN1
ATMUNX1
ATN9_1
ATRE1
ATREP1
ATREP7
ATREP10A
ATREP10B
ATREP10C
ATREP10D
ATREP11
ATREP11A
ATREP12
ATREP13
ATREP14
ATREP15
ATREP16
ATREP17
ATREP18
ATREP19
ATREP2
ATREP2A
ATREP3
ATREP4
ATREP5
ATREP6
ATREP7
ATREP8
ATREP9
ATSINE2A
ATSINE4
ATTIR16T3A
ATTIRTA1
ATTIRX1A
ATTIRX1B
ATTIRX1C
BOMZH1
BOMZH2
BRODYAGA1
BRODYAGA1A
BRODYAGA2
DT1
HARBINGER
HELITRON1
HELITRON10
HELITRON2
HELITRON3
HELITRON4
HELITRON5
HELITRONY1A
HELITRONY1B
HELITRONY1C
HELITRONY1D
HELITRONY1E
HELITRONY2
HELITRONY3
HELITRONY3A
LIMPET1
META1
RathE1_cons
RathE2_cons
RathE3_cons
ROMANIAT5
RP1_AT
SIMPLEHAT1
SIMPLEHAT6
SIMPLEHAT7
SIMPLEHAT2
TA11
TAG1
TAG2
TAG3N1
TAT1_ATH
TNAT1A
TNAT2A
TSGL
Unassigned
VANDAL1
VANDAL12
VANDAL13
VANDAL14
VANDAL16
VANDAL17
VANDAL18NA
VANDAL1N1
VANDAL2
VANDAL20
VANDAL21
VANDAL22
VANDAL2N1
VANDAL3
VANDAL4
VANDAL5
VANDAL5A
VANDAL6
VANDAL7
VANDAL8
VANDAL9
VANDALNX2
TE Family

996 **Figure 2 - figure supplement 5. TE variant enrichment and depletion for all TE families**

997 The percentage of TE variants by TE families were compared to the percentage expected due
998 to the genomic frequency of elements of each TE family. Families with more TE
999 presence/absence variants than expected are plotted in red, indicating percentage enrichment
1000 of those elements, while those with a lower number of TE variants than expected are plotted in
1001 blue, indicating percentage depletion for that TE family.

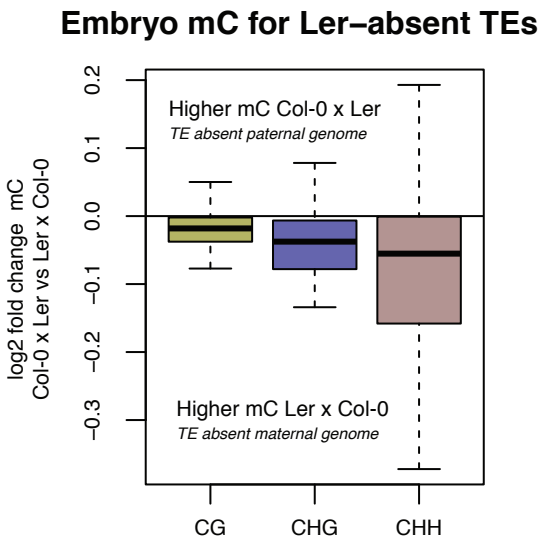
Embryo mC for Ler−absent TEs
log2 fold change mC
Col-0 x Ler vs Ler x Col-0
0.2
0.1
0.0
−0.1
−0.2
−0.3
Higher mC Col-0 x Ler
TE absent paternal genome
Higher mC Ler x Col-0
TE absent maternal genome
CG
CHG
CHH

1003 **Figure 6 - figure supplement 1. TE DNA methylation in embryos resulting from a Col-0 x**

1004 **L*er* cross**

1005 DNA methylation levels in sperm-demethylated TEs absent from L*er* but present in Col-0.

1006 Levels are $\log_2$ fold change mC/C, for each DNA methylation context, between L*er* x Col-0 and

1007 Col-0 x L*er* DNA methylation levels. Positive values indicate higher methylation in the L*er* x Col-

1008 0 (*female x male*) cross, whereas negative values represent higher methylation in the Col-0 x

1009 L*er* cross. Boxplots were constructed as for Figure 4C.

1010 # TABLES

1011 **Table 1. Mapping of paired-end reads providing evidence for TE presence/absence**
1012 **variants in L*er* to Col-0 and L*er* reference genomes.**

	Concordant	Discordant	Split	Unmapped	Total
Col-0 mapped	0	993	9,513	0	10,206
Ler mapped	10,073	92	34	7	10,206

1013

1014 **Table 2. Significantly differentially expressed genes dependent on TE presence/absence.**

TE insertion point	AGI	Gene name	Function	Pearson correlation	log2 fold change FPKM	p-value	q-value
Exon	AT1G28620	-	Lipase	0.27	-3.71	2.74E-06	1.73E-04
	AT1G31580	*ECS1*	Cell wall protein related to Xanthomonas campestris pv. campestris resistance	0.28	-2.91	9.43E-10	2.49E-07
	AT1G48820	-	Terpenoid cyclase	0.27	-2.66	1.86E-05	7.46E-04
	AT2G15040	*AtRLP18*	Disease resistance protein	0.49	-1.62	5.80E-10	2.42E-07
	AT2G16520	-	-	-0.53	3.07	1.76E-10	9.05E-08
	AT2G16810	-	F-box protein	-0.48	2.36	1.86E-05	7.46E-04
	AT3G19520	-	-	0.68	-2.61	9.98E-08	1.14E-05
	AT3G26230	*CYP71B24*	Cytochrome P450	0.53	-2.40	6.44E-13	6.63E-10
	AT3G46482	-	-	-0.48	4.46	2.05E-09	4.52E-07
	AT3G62460	-	Putative endonuclease	0.20	-2.56	9.03E-08	1.12E-05
	AT4G05500	-	F-box protein	-0.44	1.26	5.13E-06	2.66E-04
	AT4G15056	-	-	-0.60	4.63	4.25E-06	2.34E-04
	AT5G16990	-	Oxidative stress tolerance	-0.49	1.02	5.26E-06	2.66E-04
	AT5G38565	-	F-box protein	0.35	-1.84	2.13E-06	1.44E-04
	AT5G67310	*CYP81G1*	Cytochrome P450	0.22	-3.53	3.61E-07	3.47E-05
Intron	AT1G48820	-	Terpenoid cyclase	0.27	-2.66	1.86E-05	7.46E-04
	AT1G52710	-	Cytochrome-c oxidase activity	0.30	-2.57	8.30E-06	4.07E-04
	AT2G03913	-	Defensin-like family protein	-0.72	8.35	1.64E-17	5.06E-14
	AT3G59190	-	F-box protein	0.29	-3.39	4.13E-09	8.50E-07
	AT3G62460	-	Putative endonuclease	0.20	-2.56	9.03E-08	1.12E-05
	AT4G15056	-	-	-0.60	4.63	4.25E-06	2.34E-04
3' UTR	AT5G38565	-	F-box protein	0.35	-1.84	2.13E-06	1.44E-04
5' UTR	AT1G31580	*ECS1*	Cell wall protein related to Xanthomonas campestris pv. campestris resistance	0.28	-2.91	9.43E-10	2.49E-07
	AT2G16810	-	F-box protein	-0.48	2.36	1.86E-05	7.46E-04
	AT5G16990	-	Oxidative stress tolerance	-0.49	1.02	5.26E-06	2.66E-04
Upstream	AT1G48700	-	Oxidoreductase activity	-0.42	1.56	4.31E-07	3.91E-05
	AT1G61415	-	-	-0.38	1.90	8.52E-07	6.74E-05
	AT2G01360	-	PPR protein	-0.84	5.06	1.80E-07	1.80E-05
	AT2G16520	-	-	-0.53	3.07	1.76E-10	9.05E-08
	AT2G16530	*PPRD2*	Oxidoreductase activity	0.42	-1.01	1.05E-07	1.16E-05
	AT2G17080	-	-	-0.49	2.65	1.15E-08	1.97E-06
	AT2G25510	-	-	0.43	-2.49	2.52E-08	3.89E-06
	AT4G11290	*AtPrx39*	Peroxidase activity, cold	0.35	-1.43	2.15E-06	1.44E-04

			tolerance				
	AT4G15620	*CASPL1E2*	-	0.38	-1.70	3.29E-08	4.61E-06
	AT5G28010	-	Defence response	0.38	-1.76	9.69E-10	2.49E-07
	AT5G32620	-	-	-0.36	2.27	3.03E-08	4.45E-06
	AT5G38565	-	F-box protein	0.35	-1.84	2.13E-06	1.44E-04
	AT5G49500	-	Signal recognition particle	-0.41	1.62	2.29E-05	8.93E-04
	AT5G66660	-	-	-0.39	1.03	1.55E-05	7.03E-04
Downstream	AT1G02770	-	-	-0.46	1.36	3.71E-07	3.47E-05
	AT1G33930	-	GTP binding	0.55	-2.61	3.57E-15	5.51E-12
	AT1G77960	-	-	0.15	-4.51	4.22E-06	2.34E-04
	AT2G12460	-	-	0.29	-2.65	7.07E-07	5.74E-05
	AT2G16810	-	F-box protein	-0.48	2.36	1.86E-05	7.46E-04
	AT2G19400	-	Kinase	0.42	-1.54	1.40E-06	1.08E-04
	AT2G27650	-	Ubiquitin thiolesterase activity	-0.41	1.20	7.88E-06	3.93E-04
	AT3G46482	-	-	-0.48	4.46	2.05E-09	4.52E-07
	AT4G03050	*AOP3*	Glucosinolate biosynthesis	-0.38	2.39	4.82E-07	4.13E-05
	AT4G07820	-	-	0.29	-2.78	1.48E-06	1.11E-04
	AT5G16990	-	Oxidative stress tolerance	-0.49	1.02	5.26E-06	2.66E-04
	AT5G22608	-	-	0.33	-1.94	4.76E-07	4.13E-05
	AT5G23770	*AtDUF8*	-	-0.56	1.53	5.50E-07	4.59E-05
	AT5G24570	-	-	0.27	-1.01	2.43E-05	9.37E-04
	AT5G27340	-	-	-0.41	4.08	4.26E-08	5.72E-06
	AT5G35796	-	-	-0.50	1.36	7.65E-09	1.39E-06
	AT5G45840	-	Protein kinase activity	0.25	-3.22	1.51E-06	1.11E-04
	AT5G66455	-	PPR pseudogene	0.32	-1.44	1.39E-05	6.52E-04

1015
1016

1017 **Supplementary Table 1. TE superfamily enrichments for TE variants**

TE superfamily	Genomic count	Variant count	Genomic frequency	Variant frequency	Enrichment (%)
DNA	1829	798	5.86E+00	3.76E-02	-2.10
DNA/En-Spm	941	933	3.02E+00	4.40E-02	1.38
DNA/Harbinger	379	339	1.22E+00	1.60E-02	0.38
DNA/HAT	1035	1109	3.32E+00	5.23E-02	1.91
DNA/Mariner	151	98	4.84E-01	4.62E-03	-0.02
DNA/MuDR	5410	3777	1.73E+01	1.78E-01	0.45
DNA/Pogo	344	127	1.10E+00	5.98E-03	-0.50
DNA/Tc1	95	37	3.05E-01	1.74E-03	-0.13
LINE	81	45	2.60E-01	2.12E-03	-0.05
LINE/L1	1366	1017	4.38E+00	4.79E-02	0.41
LTR/Copia	1781	1747	5.71E+00	8.23E-02	2.52
LTR/Gypsy	4181	4442	1.34E+01	2.09E-01	7.53
RathE1_cons	213	150	6.83E-01	7.07E-03	0.02
RathE2_cons	74	14	2.37E-01	6.60E-04	-0.17
RathE3_cons	104	72	3.33E-01	3.39E-03	0.01
RC/Helitron	12945	6372	4.15E+01	3.00E-01	-11.48
SINE	131	64	4.20E-01	3.02E-03	-0.12
Unassigned	129	80	4.14E-01	3.77E-03	-0.04

1018

1019 **Supplementary Table 2. TE family enrichments for TE variants.**

TE family	Genomic count	Variant count	Genomic frequency	Variant frequency	Enrichment (%)
ARNOLD1	39	13	1.30E-01	6.48E-04	-0.06
ARNOLD2	68	42	2.26E-01	2.09E-03	-0.02
ARNOLD3	45	38	1.49E-01	1.90E-03	0.04
ARNOLD4	23	11	7.64E-02	5.49E-04	-0.02
ARNOLDY1	237	100	7.87E-01	4.99E-03	-0.29
ARNOLDY2	288	131	9.56E-01	6.53E-03	-0.30
AT9NMU1	45	68	1.49E-01	3.39E-03	0.19
AT9TSD1	55	58	1.83E-01	2.89E-03	0.11
ATCOPIA11	26	22	8.63E-02	1.10E-03	0.02
ATCOPIA13	35	31	1.16E-01	1.55E-03	0.04
ATCOPIA24	27	9	8.97E-02	4.49E-04	-0.04
ATCOPIA28	81	57	2.69E-01	2.84E-03	0.02
ATCOPIA30	33	12	1.10E-01	5.99E-04	-0.05
ATCOPIA35	22	27	7.31E-02	1.35E-03	0.06
ATCOPIA37	32	14	1.06E-01	6.98E-04	-0.04
ATCOPIA41	39	39	1.30E-01	1.95E-03	0.07
ATCOPIA42	35	17	1.16E-01	8.48E-04	-0.03
ATCOPIA43	29	18	9.63E-02	8.98E-04	-0.01
ATCOPIA45	20	14	6.64E-02	6.98E-04	0.00
ATCOPIA49	34	32	1.13E-01	1.60E-03	0.05
ATCOPIA57	48	50	1.59E-01	2.49E-03	0.09
ATCOPIA59	20	5	6.64E-02	2.49E-04	-0.04
ATCOPIA65	34	29	1.13E-01	1.45E-03	0.03
ATCOPIA66	20	10	6.64E-02	4.99E-04	-0.02
ATCOPIA68	43	14	1.43E-01	6.98E-04	-0.07
ATCOPIA69	25	36	8.30E-02	1.80E-03	0.10
ATCOPIA75	20	19	6.64E-02	9.48E-04	0.03
ATCOPIA78	24	64	7.97E-02	3.19E-03	0.24
ATCOPIA94	39	21	1.30E-01	1.05E-03	-0.02
ATCOPIA95	72	49	2.39E-01	2.44E-03	0.01
ATDNA12T3_2	660	53	2.19E+00	2.64E-03	-1.93
ATDNA12T3A	22	12	7.31E-02	5.99E-04	-0.01
ATDNA1T9A	36	11	1.20E-01	5.49E-04	-0.06
ATDNA2T9A	48	50	1.59E-01	2.49E-03	0.09
ATDNA2T9B	26	25	8.63E-02	1.25E-03	0.04
ATDNA2T9C	242	103	8.04E-01	5.14E-03	-0.29
ATDNAI26T9	25	24	8.30E-02	1.20E-03	0.04
ATDNAI27T9A	116	150	3.85E-01	7.48E-03	0.36
ATDNAI27T9B	43	49	1.43E-01	2.44E-03	0.10
ATDNAI27T9C	108	54	3.59E-01	2.69E-03	-0.09
ATDNATA1	28	36	9.30E-02	1.80E-03	0.09
ATENSPM1	30	32	9.96E-02	1.60E-03	0.06
ATENSPM10	81	61	2.69E-01	3.04E-03	0.04

ATENSPM11	47	48	1.56E-01	2.39E-03	0.08
ATENSPM1A	77	59	2.56E-01	2.94E-03	0.04
ATENSPM2	114	88	3.79E-01	4.39E-03	0.06
ATENSPM3	98	127	3.25E-01	6.33E-03	0.31
ATENSPM4	50	99	1.66E-01	4.94E-03	0.33
ATENSPM5	111	88	3.69E-01	4.39E-03	0.07
ATENSPM6	151	112	5.01E-01	5.59E-03	0.06
ATENSPM7	74	65	2.46E-01	3.24E-03	0.08
ATENSPM9	97	150	3.22E-01	7.48E-03	0.43
ATGP1	144	168	4.78E-01	8.38E-03	0.36
ATGP10	165	151	5.48E-01	7.53E-03	0.21
ATGP2	48	97	1.59E-01	4.84E-03	0.32
ATGP2N	54	77	1.79E-01	3.84E-03	0.20
ATGP3	60	36	1.99E-01	1.80E-03	-0.02
ATGP5	86	67	2.86E-01	3.34E-03	0.05
ATGP6	25	18	8.30E-02	8.98E-04	0.01
ATGP7	47	37	1.56E-01	1.85E-03	0.03
ATGP8	92	32	3.06E-01	1.60E-03	-0.15
ATGP9B	27	22	8.97E-02	1.10E-03	0.02
ATHAT1	105	32	3.49E-01	1.60E-03	-0.19
ATHAT10	35	15	1.16E-01	7.48E-04	-0.04
ATHAT3	23	72	7.64E-02	3.59E-03	0.28
ATHAT7	20	11	6.64E-02	5.49E-04	-0.01
ATHATN1	69	18	2.29E-01	8.98E-04	-0.14
ATHATN10	48	43	1.59E-01	2.14E-03	0.06
ATHATN2	46	37	1.53E-01	1.85E-03	0.03
ATHATN3	70	20	2.32E-01	9.98E-04	-0.13
ATHATN3A	20	10	6.64E-02	4.99E-04	-0.02
ATHATN4	56	12	1.86E-01	5.99E-04	-0.13
ATHATN5	42	8	1.39E-01	3.99E-04	-0.10
ATHATN6	43	71	1.43E-01	3.54E-03	0.21
ATHATN7	71	50	2.36E-01	2.49E-03	0.01
ATHILA	198	229	6.58E-01	1.14E-02	0.48
ATHILA0_I	138	180	4.58E-01	8.98E-03	0.44
ATHILA2	413	618	1.37E+00	3.08E-02	1.71
ATHILA3	243	296	8.07E-01	1.48E-02	0.67
ATHILA4	250	265	8.30E-01	1.32E-02	0.49
ATHILA4A	310	254	1.03E+00	1.27E-02	0.24
ATHILA4B_LTR	143	234	4.75E-01	1.17E-02	0.69
ATHILA4C	206	183	6.84E-01	9.13E-03	0.23
ATHILA4D_LTR	106	47	3.52E-01	2.34E-03	-0.12
ATHILA5	131	172	4.35E-01	8.58E-03	0.42
ATHILA6A	247	331	8.20E-01	1.65E-02	0.83
ATHILA6B	134	131	4.45E-01	6.53E-03	0.21
ATHILA7	134	46	4.45E-01	2.29E-03	-0.22

ATHILA7A	31	18	1.03E-01	8.98E-04	-0.01
ATHILA8A	97	77	3.22E-01	3.84E-03	0.06
ATHILA8B	78	41	2.59E-01	2.04E-03	-0.05
ATHPOGO	25	10	8.30E-02	4.99E-04	-0.03
ATHPOGON1	174	52	5.78E-01	2.59E-03	-0.32
ATHPOGON2	27	12	8.97E-02	5.99E-04	-0.03
ATHPOGON3	118	53	3.92E-01	2.64E-03	-0.13
ATIS112A	173	122	5.75E-01	6.09E-03	0.03
ATLANTYS1	153	171	5.08E-01	8.53E-03	0.34
ATLANTYS2	179	194	5.94E-01	9.68E-03	0.37
ATLANTYS3	142	126	4.72E-01	6.28E-03	0.16
ATLINE1_1	61	70	2.03E-01	3.49E-03	0.15
ATLINE1_2	41	51	1.36E-01	2.54E-03	0.12
ATLINE1_3A	160	95	5.31E-01	4.74E-03	-0.06
ATLINE1_4	102	39	3.39E-01	1.95E-03	-0.14
ATLINE1_5	91	52	3.02E-01	2.59E-03	-0.04
ATLINE1_6	129	75	4.28E-01	3.74E-03	-0.05
ATLINE1A	289	147	9.60E-01	7.33E-03	-0.23
ATLINE2	138	146	4.58E-01	7.28E-03	0.27
ATLINEIII	196	292	6.51E-01	1.46E-02	0.81
ATMU1	59	35	1.96E-01	1.75E-03	-0.02
ATMU10	87	30	2.89E-01	1.50E-03	-0.14
ATMU11	20	11	6.64E-02	5.49E-04	-0.01
ATMU2	64	65	2.13E-01	3.24E-03	0.11
ATMU5	24	10	7.97E-02	4.99E-04	-0.03
ATMU6	26	31	8.63E-02	1.55E-03	0.07
ATMU6N1	39	20	1.30E-01	9.98E-04	-0.03
ATMU7	32	32	1.06E-01	1.60E-03	0.05
ATMUN1	107	49	3.55E-01	2.44E-03	-0.11
ATMUNX1	155	39	5.15E-01	1.95E-03	-0.32
ATN9_1	65	99	2.16E-01	4.94E-03	0.28
ATRE1	22	9	7.31E-02	4.49E-04	-0.03
ATREP1	498	390	1.65E+00	1.95E-02	0.29
ATREP10	63	51	2.09E-01	2.54E-03	0.05
ATREP10A	279	85	9.27E-01	4.24E-03	-0.50
ATREP10B	491	150	1.63E+00	7.48E-03	-0.88
ATREP10C	123	41	4.08E-01	2.04E-03	-0.20
ATREP10D	1295	489	4.30E+00	2.44E-02	-1.86
ATREP11	841	339	2.79E+00	1.69E-02	-1.10
ATREP11A	95	72	3.15E-01	3.59E-03	0.04
ATREP12	22	72	7.31E-02	3.59E-03	0.29
ATREP13	106	110	3.52E-01	5.49E-03	0.20
ATREP14	47	30	1.56E-01	1.50E-03	-0.01
ATREP15	1003	331	3.33E+00	1.65E-02	-1.68
ATREP16	47	103	1.56E-01	5.14E-03	0.36

ATREP17	34	9	1.13E-01	4.49E-04	-0.07
ATREP18	391	298	1.30E+00	1.49E-02	0.19
ATREP19	189	42	6.28E-01	2.09E-03	-0.42
ATREP2	164	306	5.45E-01	1.53E-02	0.98
ATREP2A	116	135	3.85E-01	6.73E-03	0.29
ATREP3	1439	878	4.78E+00	4.38E-02	-0.40
ATREP4	832	239	2.76E+00	1.19E-02	-1.57
ATREP5	624	237	2.07E+00	1.18E-02	-0.89
ATREP6	181	90	6.01E-01	4.49E-03	-0.15
ATREP7	164	114	5.45E-01	5.69E-03	0.02
ATREP8	75	58	2.49E-01	2.89E-03	0.04
ATREP9	201	56	6.67E-01	2.79E-03	-0.39
ATSINE2A	33	13	1.10E-01	6.48E-04	-0.04
ATSINE4	98	51	3.25E-01	2.54E-03	-0.07
ATTIR16T3A	106	71	3.52E-01	3.54E-03	0.00
ATTIRTA1	95	37	3.15E-01	1.85E-03	-0.13
ATTIRX1A	63	15	2.09E-01	7.48E-04	-0.13
ATTIRX1B	44	21	1.46E-01	1.05E-03	-0.04
ATTIRX1C	39	93	1.30E-01	4.64E-03	0.33
ATTIRX1D	28	9	9.30E-02	4.49E-04	-0.05
BOMZH1	28	45	9.30E-02	2.24E-03	0.13
BOMZH2	47	27	1.56E-01	1.35E-03	-0.02
BRODYAGA1	251	87	8.34E-01	4.34E-03	-0.40
BRODYAGA1A	586	163	1.95E+00	8.13E-03	-1.13
BRODYAGA2	525	179	1.74E+00	8.93E-03	-0.85
DT1	123	62	4.08E-01	3.09E-03	-0.10
HARBINGER	90	62	2.99E-01	3.09E-03	0.01
HELITRON1	130	124	4.32E-01	6.18E-03	0.19
HELITRON2	194	89	6.44E-01	4.44E-03	-0.20
HELITRON3	53	54	1.76E-01	2.69E-03	0.09
HELITRON4	199	79	6.61E-01	3.94E-03	-0.27
HELITRON5	56	89	1.86E-01	4.44E-03	0.26
HELITRONY1A	271	165	9.00E-01	8.23E-03	-0.08
HELITRONY1B	414	146	1.37E+00	7.28E-03	-0.65
HELITRONY1C	120	73	3.98E-01	3.64E-03	-0.03
HELITRONY1D	756	273	2.51E+00	1.36E-02	-1.15
HELITRONY1E	447	196	1.48E+00	9.78E-03	-0.51
HELITRONY2	198	73	6.58E-01	3.64E-03	-0.29
HELITRONY3	1399	646	4.65E+00	3.22E-02	-1.42
HELITRONY3A	49	92	1.63E-01	4.59E-03	0.30
LIMPET1	116	58	3.85E-01	2.89E-03	-0.10
META1	138	202	4.58E-01	1.01E-02	0.55
RathE1_cons	213	150	7.07E-01	7.48E-03	0.04
RathE2_cons	74	14	2.46E-01	6.98E-04	-0.18
RathE3_cons	104	72	3.45E-01	3.59E-03	0.01

ROMANIAT5	49	30	1.63E-01	1.50E-03	-0.01
RP1_AT	87	102	2.89E-01	5.09E-03	0.22
SIMPLEGUY1	116	155	3.85E-01	7.73E-03	0.39
SIMPLEHAT1	56	83	1.86E-01	4.14E-03	0.23
SIMPLEHAT2	73	80	2.42E-01	3.99E-03	0.16
TA11	157	49	5.21E-01	2.44E-03	-0.28
TAG1	28	2	9.30E-02	9.98E-05	-0.08
TAG2	86	127	2.86E-01	6.33E-03	0.35
TAG3N1	97	399	3.22E-01	1.99E-02	1.67
TAT1_ATH	87	117	2.89E-01	5.84E-03	0.29
TNAT1A	162	51	5.38E-01	2.54E-03	-0.28
TNAT2A	38	31	1.26E-01	1.55E-03	0.03
TSCL	81	45	2.69E-01	2.24E-03	-0.04
Unassigned	113	61	3.75E-01	3.04E-03	-0.07
VANDAL1	80	42	2.66E-01	2.09E-03	-0.06
VANDAL12	37	20	1.23E-01	9.98E-04	-0.02
VANDAL13	38	54	1.26E-01	2.69E-03	0.14
VANDAL14	25	66	8.30E-02	3.29E-03	0.25
VANDAL16	42	87	1.39E-01	4.34E-03	0.29
VANDAL17	178	128	5.91E-01	6.38E-03	0.05
VANDAL18NA	24	15	7.97E-02	7.48E-04	0.00
VANDAL1N1	52	86	1.73E-01	4.29E-03	0.26
VANDAL2	43	47	1.43E-01	2.34E-03	0.09
VANDAL20	51	56	1.69E-01	2.79E-03	0.11
VANDAL21	64	119	2.13E-01	5.94E-03	0.38
VANDAL22	48	94	1.59E-01	4.69E-03	0.31
VANDAL2N1	51	63	1.69E-01	3.14E-03	0.14
VANDAL3	177	152	5.88E-01	7.58E-03	0.17
VANDAL4	102	68	3.39E-01	3.39E-03	0.00
VANDAL5	85	56	2.82E-01	2.79E-03	0.00
VANDAL5A	56	33	1.86E-01	1.65E-03	-0.02
VANDAL6	89	95	2.96E-01	4.74E-03	0.18
VANDAL7	36	31	1.20E-01	1.55E-03	0.04
VANDAL8	123	198	4.08E-01	9.88E-03	0.58
VANDAL9	43	24	1.43E-01	1.20E-03	-0.02
VANDALNX2	37	19	1.23E-01	9.48E-04	-0.03